

## Energy localization on $q$ -tori, long-term stability, and the interpretation of Fermi-Pasta-Ulam recurrences

H. Christodoulidi,<sup>1,\*</sup> C. Efthymiopoulos,<sup>2,†</sup> and T. Bountis<sup>1,‡</sup><sup>1</sup>*Department of Mathematics, University of Patras, Patras, Greece*<sup>2</sup>*Research Center for Astronomy and Applied Mathematics, Academy of Athens, Athens, Greece*

(Received 24 April 2009; revised manuscript received 24 September 2009; published 19 January 2010)

We focus on two approaches that have been proposed in recent years for the explanation of the so-called Fermi-Pasta-Ulam (FPU) paradox, i.e., the persistence of energy localization in the “low- $q$ ” Fourier modes of Fermi-Pasta-Ulam nonlinear lattices, preventing equipartition among all modes at low energies. In the first approach, a low-frequency fraction of the spectrum is initially excited leading to the formation of “natural packets” exhibiting exponential stability, while in the second, emphasis is placed on the existence of “ $q$  breathers,” i.e., periodic continuations of the linear modes of the lattice, which are exponentially localized in Fourier space. Following ideas of the latter, we introduce in this paper the concept of “ $q$ -tori” representing exponentially localized solutions on *low-dimensional tori* and use their stability properties to reconcile these two approaches and provide a more complete explanation of the FPU paradox.

DOI: 10.1103/PhysRevE.81.016210

PACS number(s): 05.45.–a, 63.20.Ry

### I. INTRODUCTION

In a number of recent papers, Flach and co-workers [1–3] discussed the role of simple periodic solutions, called  $q$  breathers, in the dynamics of the  $\alpha$  and  $\beta$  versions of the Fermi-Pasta-Ulam (FPU) model with fixed boundaries. A  $q$  breather is the continuation, for  $\alpha \neq 0$  or  $\beta \neq 0$ , of the simple harmonic motion exhibited by the  $q$ th mode in the uncoupled case ( $\alpha = \beta = 0$ ) and implies motion by a unique frequency, which is nearly equal to the frequency of the  $q$ th mode in the uncoupled case. For small values of the coupling parameters (and the energy), the distribution of energy in  $q$  breathers stays localized in practice upon only a few modes. Thus,  $q$  breathers offer insight in understanding the problem of energy localization, as well as the long-term deviations from equipartition of the energy among the modes, i.e., the origin of the FPU paradox [4]. (For a recent and comprehensive review on discrete breathers see [5].)

Analytical estimates of various scaling laws concerning  $q$  breathers can be obtained via the method of Poincaré-Lindstedt series [1,2]. In particular, expanding the solutions for all the canonical variables up to the lowest nontrivial order with respect to the small parameters yields an exponentially decaying function for the average harmonic energy of the  $q$ th mode,  $E(q) \propto \exp(-bq)$ . The value of  $b$  depends on (i)  $\alpha$  and/or  $\beta$ , (ii) the number of degrees of freedom  $N$ , and (iii) the total energy  $E$  given to the system. The most important property of the  $q$  breathers is that their energy profiles  $E(q)$  are quite similar to those of “FPU trajectories,” i.e., solutions generated by initially exciting one or a few low- $q$  modes, whose *exponential localization* has been noted since a long time ago [6–9]. On the basis of this similarity it has been conjectured that there is a close connection between  $q$  breathers and the energy localization properties of FPU tra-

jectories. It is intriguing, however, that this localization persists even for values of the parameters (coupling, energy, and  $N$ ) for which the corresponding  $q$ -breather solution has become *unstable*. A heuristic argument for interpreting this phenomenon was offered by Flach and Ponno [3].

Adopting a different approach, Berchiolla *et al.* [10] explored in detail the question of energy equipartition in FPU experiments where a constant (low-frequency) *fraction* of the spectrum (instead of just one mode) was initially excited. The numerical indication from this study, based on a limited range of values of  $E$  and  $N$ , was that the flow of energy across the high-frequency parts of the spectrum takes place exponentially slowly, by a law of the form  $T \propto \exp(\varepsilon^{-1/4})$ , where  $T$  is the time needed for the energy to be nearly equally partitioned and  $\varepsilon = E/N$  is the specific energy of the system. In fact, this dependence appears as a piecewise power law, with different “best-fit” slopes in different ranges of values of  $\varepsilon$ . For example, a power-law behavior of the type  $T \propto \varepsilon^{-3}$  was found in a subinterval of  $\varepsilon$  values considered in [10], which fits nicely previous results on the scaling of the equipartition time with  $\varepsilon$  beyond a critical “weak chaos” threshold reported in [11]. Nevertheless, the question of whether the scaling laws characterizing the approach to equipartition depend on the total energy  $E$  or the specific energy  $E/N$  is still open, since no rigorous results have been provided so far in the literature. On the other hand, numerical results are available over a limited range of values of  $E$  and  $N$ , in which  $E$  is varied proportionally to  $N$ . Various semianalytical or numerical approaches to this question are reviewed in [12].

Interestingly enough, even if one starts by exciting *one mode* with large enough energy, one observes, long before equipartition, the formation of *metastable states* coined natural packets [13], in which the energy undergoes first a kind of equipartition among a group of low-frequency modes, as if a fraction of the spectrum (instead of one mode) was initially excited. We may thus conclude that the phenomenon of metastability characterizes FPU trajectories resulting from all types of initial excitations of the low-frequency part of

\*hchrist@master.math.upatras.gr

†cefthim@academyofathens.gr

‡bountis@math.upatras.gr

the spectrum (see [14] for a review of the “history” of the metastability scenario in the FPU problem). Furthermore, empirical scaling laws can be established [13] concerning the dependence of the “width” of a packet on the specific energy  $\varepsilon$ . These are consistent with the laws of energy localization obtained via either a continuous Hamiltonian model which interpolates the FPU dynamics in the space of Fourier modes [15,16] or the  $q$ -breather model [3]. A difference, however, between the two models is that in the framework of the continuous model the constant  $b$  in  $E(q) \propto \exp(-bq)$  turns out to be independent of  $E$ .

The results reported in the present paper aim to provide a more complete explanation of the FPU paradox of energy nonequipartition by reconciling the presence of  $q$  breathers and their induced energy localization on one hand, with the occurrence of metastable packets of low-frequency modes on the other hand. To extend the results obtained for FPU trajectories in [10,11], let us observe that the packet of modes excited in these experiments corresponds to the modes with spectral numbers satisfying the condition  $(N+1)/64 \leq q \leq 5(N+1)/64$ , with  $N$  equal to a power of 2 minus 1. For simplicity, let us alter this slightly and consider, instead, the condition  $1 \leq q \leq 4N/64$ , with  $N$  a power of 2. The lowest possible value of  $N$  allowed is  $N=16$ , for which the above condition implies that only the  $q=1$  mode is initially excited, giving a solution close to a  $q$  breather, which is an orbit lying on an invariant *one-torus* of the system. Now, if  $N$  is doubled ( $N=32$ ), the same condition implies that modes  $q=1$  and 2 may now be excited, meaning that the resulting FPU trajectories may be regarded as lying close to invariant *two-tori* of the system  $N=32$ . In general, for  $N=16s$ , the modes  $q=1, 2, \dots, s$  are initially excited and the motion should be regarded as lying close to an invariant  $s$ -torus of the system. The same holds true when natural packets of width  $s$  are formed in experiments in which the initial conditions are as adopted in [13].

This leads to the idea that the properties of the FPU trajectories could be understood by considering *classes* of special solutions lying not only on one-dimensional tori (as is the case with  $q$  breathers), but also on tori of *any low dimension*  $s \ll N$ , i.e., solutions with  $s$  independent frequencies, representing the continuation of motions resulting from exciting  $s$  modes of the uncoupled case. Generalizing the concept of  $q$  breathers, we call  $q$ -tori the quasiperiodic solutions on such low-dimensional tori. The main body of the present paper, therefore, focuses on exploring the properties of these  $q$ -tori solutions, both analytically and numerically. In particular, we establish for  $q$ -tori energy localization laws analogous to those for  $q$  breathers, using a semianalytical approach. Our numerical experiments then show that such laws describe accurately the properties not only of exact  $q$ -tori solutions, but also of FPU trajectories with nearby initial conditions.

Our work shares a common starting point with a recent paper by Giorgilli and Muraro [17], where the authors also explored the idea of FPU trajectories being confined on lower-dimensional manifolds embedded in the  $2N$ -dimensional FPU phase space. Their main result, proving that the confinement persists for times exponentially long in the inverse of  $\varepsilon$ , is obtained in the spirit of the theory of

Nekhoroshev ([18]; see also [19]), using a variant of the formulation of the Nekhoroshev theorem for “isochronous” systems [20–24]. In fact, the theory of Nekhoroshev appears to offer quite a natural framework for studying analytically the metastability scenario.

However, as has been pointed out quite early [25] a naive application of the Nekhoroshev theory in the FPU problem would break down as  $N \rightarrow \infty$  since, under the assumption that the Nekhoroshev time  $T$  depends on the specific energy  $\varepsilon$ , in the estimates  $T \sim \exp(1/\varepsilon^c)$  of the theory the exponent is of the form  $c = O(1/N)$  (see [24] for a heuristic explanation). This bad dependence of  $c$  on  $N$  actually implies that  $T = O(1)$  as  $N \rightarrow \infty$ ; hence, Nekhoroshev’s theory fails to predict long times for equipartition in that limit (a relevant theoretical result has only been obtained in lattices where a clear separation of the frequencies occurs into low and high bands; the low frequencies then become small parameters, see [26]). In [17] one has instead  $c = O(1/m)$ , where  $m$  is one half the dimension of the lower-dimensional manifold where confined FPU trajectories are expected to lie. This constitutes a significant improvement with respect to previous estimates, but still does not explain the natural packets correctly since the latter’s width was found in numerical experiments to vary as  $m \propto \varepsilon^{1/4} N$  [13], i.e., proportionally to  $N$ , for fixed  $\varepsilon$ .

Our analytical theory relies on the use of the *Poincaré-Lindstedt* method, through which we find scaling laws for the energy profile  $E(q)$  of a trajectory lying exactly on a  $q$ -torus. The consistency of the Poincaré-Lindstedt construction on a Cantor set of perturbed frequencies (or amplitudes) is explicitly demonstrated. Numerically, we find that energy localization persists for appreciably long times, for trajectories neighboring a  $q$ -torus, even beyond the energy threshold where the  $q$ -torus becomes linearly unstable. The determination of linear stability for an  $s$ -dimensional torus ( $s > 1$ ) is, of course, a subtle question since no straightforward application of the Floquet theory is available, as in the  $s=1$  case. Nevertheless, by employing an effective and reliable criterion for the stability of  $q$ -tori via the use of the recently developed method of “generalized alignment indices” (GALIs, see [27]), we are able to determine approximate critical parameter values at which a low-dimensional torus turns unstable, in the sense that orbits in its vicinity display a chaotic behavior.

It is important to remark at this point that, although the Poincaré-Lindstedt approach is quite distinct from the Birkhoff method used in the Nekhoroshev theory, it appears that the properties of exponential localization can be exploited to demonstrate (by the subsequent use of the Birkhoff method) an even better behavior of the exponent  $c$  of Nekhoroshev estimates than can be found in the literature so far. A detailed exploration of this issue is deferred to a separate study. Nevertheless, a heuristic argument offered in the closing section of this paper suggests that the removal of the dependence of  $c$  on the number of degrees of freedom is possible, at least for trajectories close to  $q$  breathers.

Our paper is structured as follows. Section II presents our analytical results on the existence and scaling laws of the  $q$ -tori. We deal here only with the  $\beta$  case, but our approach can be readily extended to the  $\alpha$  case as well. We focus on the specific and most relevant subset of  $q$ -tori corresponding

to zeroth-order excitations of a set of adjacent modes  $q_{0,i}=i$  (with  $i=1, \dots, s$ ), whose energy profile  $E(q)$  is calculated analytically. Next, our analytical predictions are tested against numerical integration of specific orbits. Section III examines the question of stability of  $q$ -tori and the persistence of energy localization of the FPU trajectories when the linear stability of the “underlying”  $q$ -tori is lost. Finally, we deal with the question of the long-term stability of exponentially localized FPU trajectories, via heuristic estimates inspired by Nekhoroshev’s theory. Section IV summarizes the main conclusions of the present study.

## II. EXISTENCE AND STABILITY OF $q$ -TORI

### A. FPU $\beta$ model

The  $\beta$ -FPU Hamiltonian for a lattice of  $N$  particles reads

$$H = \frac{1}{2} \sum_{k=1}^N y_k^2 + \frac{1}{2} \sum_{k=0}^N (x_{k+1} - x_k)^2 + \frac{\beta}{4} \sum_{k=0}^N (x_{k+1} - x_k)^4, \quad (1)$$

where  $x_k$  is the  $k$ th particle’s displacement with respect to the equilibrium position and  $y_k$  is its canonically conjugate momentum. Fixed boundary conditions are defined by setting  $x_0 = x_{N+1} = 0$ .

The normal-mode canonical variables  $(Q_q, P_q)$  are introduced by the linear canonical transformations

$$\begin{aligned} x_k &= \sqrt{\frac{2}{N+1}} \sum_{q=1}^N Q_q \sin\left(\frac{qk\pi}{N+1}\right), \\ y_k &= \sqrt{\frac{2}{N+1}} \sum_{q=1}^N P_q \sin\left(\frac{qk\pi}{N+1}\right). \end{aligned} \quad (2)$$

Substitution of Eq. (2) into Eq. (1) yields the Hamiltonian in the form  $H = H_2 + H_4$  in which the quadratic part is diagonal,

$$H_2 = \sum_{q=1}^N \frac{P_q^2 + \Omega_q^2 Q_q^2}{2}, \quad (3)$$

with normal-mode frequencies

$$\Omega_q = 2 \sin\left(\frac{q\pi}{2(N+1)}\right), \quad 1 \leq q \leq N. \quad (4)$$

The quartic part of the Hamiltonian reads

$$H_4 = \frac{\beta}{2(N+1)} \sum_{q,l,m,n=1}^N C_{q,l,m,n} \Omega_q \Omega_l \Omega_m \Omega_n Q_q Q_l Q_m Q_n, \quad (5)$$

where the coefficients  $C_{q,l,m,n}$  take nonzero values only for particular combinations of the indices  $q, l, m, n$ , namely,

$$C_{q,l,m,n} = \begin{cases} 1 & \text{if } q \pm l \pm m \pm n = 0 \\ -1 & \text{if } q \pm l \pm m \pm n = \pm 2(N+1), \end{cases} \quad (6)$$

in which all possible combinations of the  $\pm$  signs are taken into account. Thus, in the new canonical variables, the equations of motion are

$$\ddot{Q}_q + \Omega_q^2 Q_q = - \frac{\beta}{2(N+1)} \sum_{l,m,n=1}^N C_{q,l,m,n} \Omega_q \Omega_l \Omega_m \Omega_n Q_l Q_m Q_n. \quad (7)$$

If  $\beta=0$ , the individual harmonic energies  $E_q = (P_q^2 + \Omega_q^2 Q_q^2)/2$  are preserved by Eq. (7), i.e., the energies  $E_q$  form a set of  $N$  integrals in involution. When  $\beta \neq 0$ , however, the harmonic energies become functions of time and only the total energy  $E = \sum_{q=1}^N E_q(t)$  is conserved. The specific energy is then defined as  $\varepsilon = E/N$ , while the average harmonic energy of each mode over a time interval  $0 \leq t \leq T$  is given by the integral  $\bar{E}_q(T) = \frac{1}{T} \int_0^T E_q(t) dt$ .

In classical FPU experiments, one starts with the total energy shared only by a small subset of modes. Then, for short time intervals  $T$ , we have  $E_q(T) \approx 0$  for all  $q$  corresponding to nonexcited modes. Equipartition means that, due to the nonlinear terms, the energy will eventually be shared equally by all modes, i.e.,

$$\lim_{T \rightarrow \infty} \bar{E}_q(T) = \varepsilon, \quad q = 1, \dots, N. \quad (8)$$

The usual ergodic assumption of statistical mechanics leads to the conclusion that Eq. (8) is violated only for orbits resulting from a zero measure set of initial conditions. The FPU paradox owes its name to the crucial observation that large deviations from the approximate equality  $\bar{E}_q(T) \approx \varepsilon$  occur for many other orbits as well. Depending on the initial conditions, these deviations are termed “FPU recurrences” and are seen to persist even when  $T$  becomes very large.

### B. $q$ -tori and their construction by Poincaré-Lindstedt series

From the above discussion, one infers that the dynamics of FPU recurrences is governed by particular solutions of the FPU equations (7) for which energy localization occurs only on a small subset of Fourier modes. Such solutions lie on *tori of low dimensionality*, which we shall henceforth call  $q$ -tori since they also turn out to be exponentially localized in Fourier space, like the  $q$ -breather solutions discussed in [1,2].

We now introduce the main ingredients of our method of  $q$ -torus construction, using an explicitly solved example for  $N=8$ , whose solutions lie on a two-dimensional torus representing the continuation, for  $\beta \neq 0$ , of the quasiperiodic solution of the uncoupled ( $\beta=0$ ) system  $Q_1(t) = A_1 \cos \Omega_1 t$ ,  $Q_2(t) = A_2 \cos \Omega_2 t$ , for a suitable choice of  $A_1$  and  $A_2$ .

To this end, we follow the Poincaré-Lindstedt method and look for solutions  $Q_q(t)$  (with  $q=1, \dots, 8$ ) expanded as a series in the parameter  $\sigma = \beta/2(N+1)$ , namely,

$$Q_q(t) = Q_q^{(0)}(t) + \sigma Q_q^{(1)}(t) + \sigma^2 Q_q^{(2)}(t) + \dots, \quad q = 1, \dots, 8. \quad (9)$$

For the motion to be quasiperiodic on a two-torus, the functions  $Q_q^{(r)}(t)$  must, at any order  $r$ , be trigonometric polynomials involving only two frequencies (and their multiples). Furthermore, for the motion to represent a continuation of the unperturbed solutions  $Q_1$  and  $Q_2$ , the frequencies  $\omega_1$  and

$\omega_2$  must be small corrections of the normal-mode frequencies  $\Omega_1$  and  $\Omega_2$ . According to the Poincaré-Lindstedt method, these new frequencies are also given by a series in powers of  $\sigma$ , as

$$\omega_q = \Omega_q + \sigma\omega_q^{(1)} + \sigma^2\omega_q^{(2)} + \dots, \quad q = 1, 2. \quad (10)$$

The corrections are determined by the requirement that all terms in the differential equations of motion, giving rise to secular terms (of the form  $t \sin \omega_q t$ , etc.) in the solutions  $Q_q(t)$ , be eliminated.

Let us consider the equation of motion for the first mode, whose first few terms on the right-hand side (r.h.s) are

$$\ddot{Q}_1 + \Omega_1^2 Q_1 = -\sigma(3\Omega_1^4 Q_1^3 + 6\Omega_1^2 \Omega_2^2 Q_1 Q_2^2 + 3\Omega_1^3 \Omega_3 Q_1^2 Q_3 + \dots). \quad (11)$$

Proceeding with the Poincaré-Lindstedt series, the frequency  $\Omega_1$  is substituted on the left-hand side (l.h.s.) of Eq. (11) by its equivalent expression obtained by squaring Eq. (10) and solving for  $\Omega_1^2$ . Up to first order in  $\sigma$  this gives

$$\Omega_1^2 = \omega_1^2 - 2\sigma\Omega_1\omega_1^{(1)} + \dots. \quad (12)$$

Substituting expansions (9) into Eq. (11), as well as the frequency expansion (12) into the l.h.s. of Eq. (11), and grouping together terms of like orders, we find at zeroth order  $\ddot{Q}_1^{(0)} + \omega_1^2 Q_1^{(0)} = 0$ , while at first order

$$\ddot{Q}_1^{(1)} + \omega_1^2 Q_1^{(1)} = 2\Omega_1\omega_1^{(1)}Q_1^{(0)} - 3\Omega_1^4(Q_1^{(0)})^3 - 6\Omega_1^2\Omega_2^2Q_1^{(0)} \times (Q_2^{(0)})^2 - 3\Omega_1^3\Omega_3(Q_1^{(0)})^2Q_3^{(0)} + \dots. \quad (13)$$

Repeating the above procedure for modes 2 and 3, we find that their zeroth-order equations also take the harmonic-oscillator form

$$\ddot{Q}_2^{(0)} + \omega_2^2 Q_2^{(0)} = 0, \quad \ddot{Q}_3^{(0)} + \Omega_3^2 Q_3^{(0)} = 0. \quad (14)$$

Note that the *corrected* frequencies  $\omega_1$  and  $\omega_2$  appear in the zeroth-order equations for modes 1 and 2, while the *uncorrected* frequency  $\Omega_3$  appears in the zeroth-order equation of mode 3 (similarly,  $\Omega_4, \dots, \Omega_8$  appear in the zeroth-order equations of modes 4–8). Continuing the construction of a solution which lies on a two-torus, we start from particular solutions of Eq. (14) (with zero velocities at  $t=0$ ) which read

$$Q_1^{(0)}(t) = A_1 \cos \omega_1 t, \quad Q_2^{(0)}(t) = A_2 \cos \omega_2 t,$$

$$Q_3^{(0)}(t) = A_3 \cos \Omega_3 t,$$

where the amplitudes  $A_1, A_2, A_3$  are arbitrary. If the solution is to lie on a two-torus with frequencies  $\omega_1$  and  $\omega_2$ , we must set  $A_3=0$ , so that no third frequency is introduced in the solutions. In the same way, the zeroth-order equations  $\ddot{Q}_q^{(0)} + \Omega_q^2 Q_q^{(0)} = 0$  for the remaining modes  $q=4, \dots, 8$  yield solutions  $Q_q^{(0)}(t) = A_q \cos \Omega_q t$  and we set  $A_4=A_5=\dots=A_8=0$ . Thus, we are left with only two nonzero free amplitudes  $A_1$  and  $A_2$ .

Now, consider Eq. (13) for the first-order term  $Q_1^{(1)}(t)$ . Only zeroth-order terms  $Q_q^{(0)}(t)$  appear on its r.h.s., allowing for the solution to be found recursively. The crucial remark is that by the choice  $A_3=\dots=A_8=0$ , one also has  $Q_3^{(0)}(t)=\dots$

$= Q_8^{(0)}(t)=0$ ; whence, only a small subset of the terms appearing in the original equations of motion survive on the r.h.s. of Eq. (13), namely, those in which none of the functions  $Q_3^{(0)}(t), \dots, Q_8^{(0)}(t)$  appears. As a result, Eq. (13) is simplified dramatically and upon substitution of  $Q_1^{(0)}(t)=A_1 \cos \omega_1 t$ ,  $Q_2^{(0)}(t)=A_2 \cos \omega_2 t$  reduces to

$$\ddot{Q}_1^{(1)} + \omega_1^2 Q_1^{(1)} = 2\Omega_1\omega_1^{(1)}A_1 \cos \omega_1 t - 3\Omega_1^4 A_1^3 \cos^3 \omega_1 t - 6\Omega_1^2 \Omega_2^2 A_1 A_2^2 \cos \omega_1 t \cos^2 \omega_2 t. \quad (15)$$

This can now be used to fix  $\omega_1^{(1)}$ , so that no secular terms appear in the solution, yielding

$$\omega_1^{(1)} = \frac{9}{8}A_1^2\Omega_1^3 + \frac{3}{2}A_2^2\Omega_1\Omega_2^2,$$

while, after some simple operations, we find for  $Q_1^{(1)}$

$$Q_1^{(1)}(t) = \frac{3A_1^3\Omega_1^4 \cos 3\omega_1 t}{32\omega_1^2} + \frac{3A_1 A_2^2 \Omega_1^2 \Omega_2^2 \cos(\omega_1 + 2\omega_2)t}{2[(\omega_1 + 2\omega_2)^2 - \omega_1^2]} + \frac{3A_1 A_2^2 \Omega_1^2 \Omega_2^2 \cos(\omega_1 - 2\omega_2)t}{2[(\omega_1 - 2\omega_2)^2 - \omega_1^2]}. \quad (16)$$

By the same analysis, we fix the frequency correction of the second mode,

$$\omega_2^{(1)} = \frac{9}{8}A_2^2\Omega_2^3 + \frac{3}{2}A_1^2\Omega_1^2\Omega_2,$$

and obtain the solution

$$Q_2^{(1)}(t) = \frac{3A_2^3\Omega_2^4 \cos 3\omega_2 t}{32\omega_2^2} + \frac{3A_1^2 A_2 \Omega_1^2 \Omega_2^2 \cos(2\omega_1 + \omega_2)t}{2[(2\omega_1 + \omega_2)^2 - \omega_2^2]} + \frac{3A_1^2 A_2 \Omega_1^2 \Omega_2^2 \cos(2\omega_1 - \omega_2)t}{2[(2\omega_1 - \omega_2)^2 - \omega_2^2]}, \quad (17)$$

which has a similar structure as the first-order solution of the first mode. For the third-order term there is no frequency correction, and we find

$$Q_3^{(1)}(t) = \frac{A_1^3 \Omega_1^3 \Omega_3}{4} \left( \frac{3 \cos \omega_1 t}{\omega_1^2 - \Omega_3^2} + \frac{\cos 3\omega_1 t}{9\omega_1^2 - \Omega_3^2} \right) + \frac{3A_1 A_2^2 \Omega_1 \Omega_2^2 \Omega_3}{4} \left( \frac{\cos(\omega_1 - 2\omega_2)t}{(\omega_1 - 2\omega_2)^2 - \Omega_3^2} + \frac{\cos(\omega_1 + 2\omega_2)t}{(\omega_1 + 2\omega_2)^2 - \Omega_3^2} + \frac{2 \cos \omega_1 t}{\omega_1^2 - \Omega_3^2} \right). \quad (18)$$

We may thus proceed to the sixth mode to find solutions in which all the functions  $Q_3^{(0)}, \dots, Q_6^{(0)}$  are equal to zero, while the functions  $Q_3^{(1)}, \dots, Q_6^{(1)}$  are nonzero. However, a new situation appears when we arrive at the seventh and eighth modes. A careful inspection of the equation for the term  $Q_7^{(1)}(t)$ ,

$$\ddot{Q}_7^{(1)} + \Omega_7^2 Q_7^{(1)} = - \sum_{l,m,n=1}^8 C_{7,l,m,n} \Omega_7 \Omega_l \Omega_m \Omega_n Q_l^{(0)} Q_m^{(0)} Q_n^{(0)}, \quad (19)$$

shows that there can be *no term* on the r.h.s. which does not involve some of the functions  $Q_3^{(0)}, \dots, Q_8^{(0)}$ . Again, this follows from the selection rules for the coefficients of Eq. (6).

Since all these functions are equal to zero, the r.h.s. of Eq. (19) is equal to zero. Taking this into account, we set  $Q_7^{(1)}(t)=0$ , so as not to introduce a third frequency  $\Omega_7$  in the solutions; whence, the series expansion (9) for  $Q_7(t)$  necessarily starts with terms of order at least  $O(\sigma^2)$ . The same holds true for the equation determining  $Q_8^{(1)}(t)$ .

Some remarks regarding the above construction are in order:

(i) *Consistency.* The solutions (16)–(18) (and those of subsequent orders) are meaningful only when the frequencies appearing in the denominators satisfy no commensurability condition. The spectrum of uncorrected frequencies  $\Omega_q$ , given by Eq. (4), is fully incommensurable only if  $N$  is either a prime number minus 1 or a power of 2 minus 1 [28]. In all other cases, there are commensurabilities among the unperturbed frequencies, examples of which are given, e.g., in [29]. However, such commensurabilities do not affect the consistency of the construction of the Poincaré-Lindstedt series, because it can be shown that no divisors of the form  $\sum_{q=1}^N n_q \Omega_q$  appear in the series at any order and for any integer vector  $\mathbf{n} \equiv (n_1, n_2, \dots, n_q) \neq (0, 0, \dots, 0)$ . The proof of this statement follows from the fact that the kernel differential equations [like Eq. (15)] determining all terms  $Q_q^{(k)}$  (with  $q=1, \dots, 8$ ) at order  $k$  read

$$\begin{aligned} \ddot{Q}_q^{(k)}(t) + \omega_q^2 Q_q^{(k)}(t) \\ = B_q^{(k)} \omega_q^{(k)} \cos \omega_q t + \sum_{\substack{n_1, n_2 \in \mathbb{Z} \\ |n_1| + |n_2| \neq 0}}^{k-1} A_{q, n_1, n_2}^{(k)} \cos[(n_1 \omega_1 + n_2 \omega_2) t] \end{aligned} \quad (20)$$

if  $q = 1, 2$ ,

while for  $q=3, \dots, 8$  the same equation holds with  $B_q^{(k)}=0$  and  $\omega_q^2$  on the l.h.s. replaced with  $\Omega_q^2$ . The coefficients  $B_q^{(k)}$  and  $A_{q, n_1, n_2}^{(k)}$  in Eq. (20) are determined at previous steps of the construction [see Eq. (24) below for arbitrary  $s$ ]. It follows, therefore, that all new divisors appearing at successive orders belong to one of the following sets:

$$(n_1 \pm 1)\omega_1 + n_2\omega_2, \quad n_1\omega_1 + (n_2 \pm 1)\omega_2,$$

$$\Omega_q \pm (n_1\omega_1 + n_2\omega_2), \quad q = 3, \dots, 8$$

for  $n_1, n_2 \in \mathbb{Z}$ ,  $|n_1| + |n_2| \neq 0$ ; whence, we deduce that no zero divisors can ever show up in the Poincaré-Lindstedt series due to commensurabilities between the unperturbed frequencies  $\Omega_q$ . On the other hand, we can also exclude the appearance of zero divisors due to the perturbed frequencies  $\omega_1, \omega_2$  if the frequencies in a quasiperiodic solution are *fixed in advance* so that the two frequencies do not belong to the countable set of all planes defined by the relations  $(n_1 \pm 1)\omega_1 + n_2\omega_2 = 0$ ,  $n_1\omega_1 + (n_2 \pm 1)\omega_2 = 0$ ,  $\Omega_q + (n_1\omega_1 + n_2\omega_2) = 0$ ,  $q=3, \dots, 8$ , for all integer values  $n_1, n_2 \in \mathbb{Z}$ ,  $|n_1| + |n_2| \neq 0$ . We stress that fixing the frequencies in advance is a necessary ingredient of the Poincaré-Lindstedt method since otherwise the equations at all orders [as, for example, Eqs. (16)–(18)] would not be solvable. Furthermore, this frequency specification is analogous to the procedure followed in the construction of Kolmogorov's normal form representing solutions on Kolmogorov-Arnold-Moser tori (see [30]

for a detailed comparison of the two methods). Since the frequencies  $\omega_1, \omega_2$  are functions of the amplitudes  $A_1, A_2$ , one deduces that the formal consistency of the method can be established in the complement of all excluded planes, i.e., a Cantor set in either the frequency space  $(\omega_1, \omega_2)$  or the amplitude space  $(A_1, A_2)$ .

The above demonstration of consistency is readily generalized to the construction of  $s$ -dimensional  $q$ -tori by the nonlinear continuation of the set of linear modes  $q_i$  (with  $i = 1, \dots, s$ ). Namely, one can demonstrate that the consistency holds on a Cantor set of amplitude multiplets  $(A_{q_1}, A_{q_2}, \dots, A_{q_s})$  such that the resulting perturbed frequencies  $\omega_{q_i}$  ( $i=1, \dots, s$ ) do not lie on any one of the planes

$$(n_1 + m_1)\omega_{q_1} + (n_2 + m_2)\omega_{q_2} + \dots + (n_s + m_s)\omega_{q_s} = 0$$

or

$$\Omega_q \pm (n_1\omega_{q_1} + n_2\omega_{q_2} + \dots + n_s\omega_{q_s}) = 0,$$

where  $q = \{1, \dots, N\} \setminus \{q_1, \dots, q_s\}$ ;  $n_1, \dots, n_s \in \mathbb{N}$ ;  $|n_1| + \dots + |n_s| \neq 0$ ; and  $m_q = -1, 0$ , or  $1$  for all  $q=1, \dots, s$ . For example, if the first  $s$  modes are excited by amplitudes  $A_k$  (with  $k=1, \dots, s$ ) the formula for the perturbed frequencies reads

$$\omega_q = \Omega_q + \frac{3\sigma}{2} \Omega_q \sum_{k=1}^s A_k^2 \Omega_k^2 - \frac{3\sigma}{8} A_q^2 \Omega_q^3 + O(\sigma^2; A_1, \dots, A_s),$$

(21)  $q=1, \dots, s$ . Fixing the values of the frequencies  $\omega_q$  in advance implies that Eq. (21) should be regarded as yielding the (unknown) amplitudes  $A_k$  for which the quasiperiodic solution exhibits the chosen set of frequencies. The case  $s=1$  implies that the same property holds for the Poincaré-Lindstedt series representing  $q$  breathers [2]. That is, while by Lyapunov's theorem the continuation of the periodic orbits is guaranteed in an open domain of values  $A_{q0}$ , the Poincaré-Lindstedt series can only be constructed on a Cantor subset of this domain. Yet, this is sufficient for our present purpose, which is to determine by a semianalytical approach scaling laws for the energy localization on  $q$ -tori (or  $q$  breathers).

(ii) *Convergence.* Even after consistency is demonstrated, no proof has yet been provided for the convergence of the series. As demonstrated in the works of Eliasson [31] and Gallavotti [32,33], the question of convergence of the Lindstedt series is notoriously difficult even in simple Hamiltonian systems. This is because the Lindstedt series for orbits on invariant tori are convergent, but not absolutely (see the review by Giorgilli [34]). On the other hand, it is possible to make an absolutely convergent classical expansion by the use of the Kolmogorov normal form as developed by Giorgilli and Locatelli [35]. Such an analysis, however, is quite cumbersome and will be deferred to another publication as it would obscure the results presented here.

Thus, we prefer to justify our previous statements by numerical simulations, taking our initial conditions from the analytical solutions (9) at  $t=0$  and using the GALI method [27] to demonstrate that the solutions lie, indeed, on two-dimensional tori, as shown in Fig. 1. The numerical solution for the modes  $Q_1(t)$ ,  $Q_3(t)$ , and  $Q_7(t)$  is checked against the

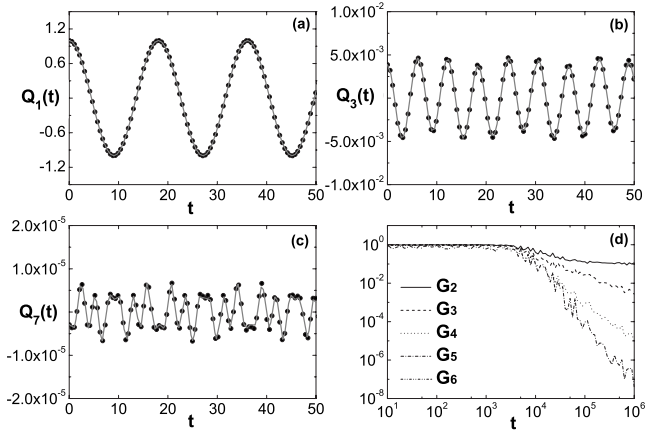


FIG. 1. Comparison of numerical (points) versus analytical (solid line) solutions, using the Poincaré-Lindstedt series up to order  $O(\sigma^2)$ , for the temporal evolution of the modes (a)  $q=1$ , (b)  $q=3$ , and (c)  $q=7$ , when  $A_1=1, A_2=0.5$  and  $N=8, \beta=0.1$  and (d) the time evolution of the GALI indices  $G_2-G_6$  up to a time  $t=10^6$  show that the motion lies on two-dimensional torus.

analytical solution via the Poincaré-Lindstedt series, truncated at second order with respect to  $\sigma$ , when  $N=8, \beta=0.1, A_1=1$ , and  $A_2=0.5$ . The size of the error is found to be precisely that expected by the truncation order in Figs. 1(a)–1(c), while in Fig. 1(d) the GALI method shows that the numerical orbit lies on a two-torus.

Let us recall that according to Skokos *et al.* [27], the GALI indicators  $G_k$  (with  $k=2,3,\dots$ ), for chaotic orbits, decay exponentially fast due to the attraction of all deviation vectors by the most unstable direction corresponding to the maximal Lyapunov exponent. On the other hand, if an orbit lies on a *stable*  $s$ -dimensional torus, the GALI indices  $G_2, \dots, G_s$  oscillate about a *nonzero* value, while the indices  $G_{s+j}$  (with  $j=1,2,\dots$ ) follows asymptotically power laws falling at least as  $t^{-j}$ .

This is precisely what we observe in Fig. 1(d). Namely, after a transient initial interval (required for phase mixing to become effective), the index  $G_2$  stabilizes at a constant value  $G_2 \approx 0.1$ , while all subsequent indices, starting from  $G_3$  decay following a power law as predicted by the theory. The time for phase mixing is estimated to be of order  $N^3/\beta \approx 10^4$ . This implies that beyond  $t=10^4$  we should observe the expected asymptotic behavior of the GALI indices to set in, as is the case in Fig. 1(d). Thus, we conclude that the motion lies on a two-torus, exactly as predicted by the Poincaré-Lindstedt construction, despite the fact that some excitation was provided initially to all modes.

(iii) *Presence and accumulation of small divisors.* There are, of course, small divisors appearing in terms of all orders beyond the zeroth. First, the low-mode frequencies satisfy  $\omega_q \sim \pi q/N$ , and hence divisors like  $\omega_1^2$  or  $(\omega_1 - 2\omega_2)^2 \pm \omega_1^2$  [appearing, e.g., in Eq. (16)] are small and care must be taken regarding their effect on the growth of terms of the series at successive orders. In fact, the most important effects are introduced by *nearly resonant* divisors, like  $9\omega_1^2 - \Omega_3^2$  in Eq. (18). Since the first-order corrections of the frequencies  $\omega_1$  and  $\omega_2$  are  $O(\beta A_j^2/N^4)$ , for  $A_j, \beta$  sufficiently small, one may still use for them the approximation given by the first

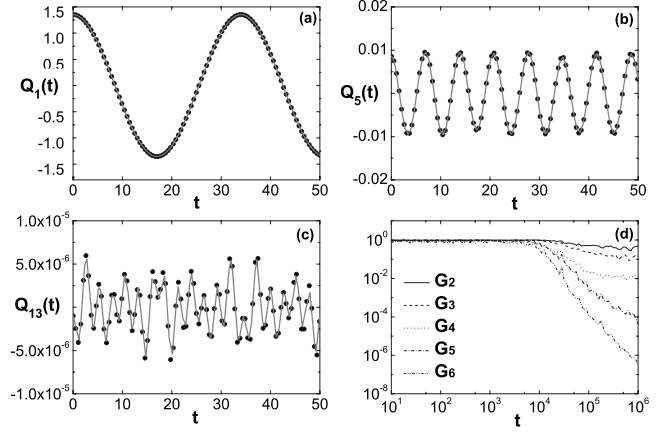


FIG. 2. Same as in Fig. 1, showing the existence of a four-torus in the system with  $N=16, \beta=0.1$ , when  $A_1=1, A_2=0.5, A_3=0.333\dots$ , and  $A_4=0.25$ . The temporal evolution  $Q_q(t)$  is shown for the modes (a)  $q=1$ , (b)  $q=5$ , and (c)  $q=13$ . (d) The GALI indices  $G_k$  (with  $k=2,3,4$ ) are seen to stabilize after  $t \sim 10^4$ , while for  $k \geq 5$  the indices continue to decrease by power laws.

two terms in the sinus expansion of Eq. (4), namely,

$$\omega_q \approx \frac{\pi q}{(N+1)} - \frac{\pi^3 q^3}{24(N+1)^3} \quad (22)$$

with the error being  $O(A_j^2 \beta/N^4)$  for  $\omega_1, \omega_2$ , and  $O((q/N)^5)$  for all other frequencies. This implies that a divisor like  $9\omega_1^2 - \Omega_3^2$  can be approximated by the relation

$$\begin{aligned} |q^2 \omega_1^2 - \Omega_3^2| &= |(q\omega_1 + \Omega_q)(q\omega_1 - \Omega_q)| \\ &\approx \frac{2q\pi}{(N+1)} \frac{\pi^3 (q^3 - q)}{24(N+1)^3} \\ &\approx \frac{\pi^4 q^4}{12N^4} + O\left(\frac{q^6}{N^6}\right). \end{aligned}$$

In general, the terms produced at consecutive orders involve products of divisors, whose influence on the size of the series terms must be taken into account in estimates of the profile of energy localization for the  $q$ -tori solutions, as explained in Sec. II D below.

(iv) *Sequence of mode excitations.* The profile of energy localization along a  $q$ -torus solution is determined by the sequence of mode excitations arising as the recursive scheme proceeds to subsequent orders. The term “excitation” here means that the solutions of the Poincaré-Lindstedt method should be nonzero for the first time at the order where it is claimed that the excitation takes place. For example, as already explained in our previous construction of a two-torus solution, modes 1 and 2 are excited at zeroth order, modes 3–6 at first order, and modes 7 and 8 at the second order of the recursive scheme.

Figure 2 presents one more example showing the comparison between our analytical and numerical results for the modes  $Q_1(t), Q_5(t)$ , and  $Q_{13}(t)$ , along a four-torus solution constructed precisely as described above, with  $N=16, \beta=0.1$  and by exciting modes 1–4 at zeroth order, via the amplitudes  $A_1=1, A_2=0.5, A_3=0.333\dots$ , and  $A_4=0.25$ . In

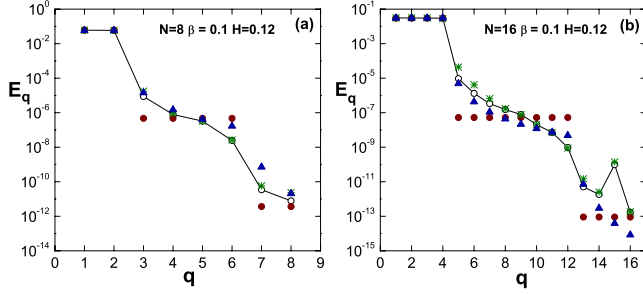


FIG. 3. (Color online) The average harmonic energy  $E_q$  of the  $q$ th mode as a function of  $q$ , after a time  $T=10^6$  for the (a) two-torus and (b) four-torus solutions (open circles) corresponding to the initial conditions used in Figs. 1 and 2, respectively. The stars are  $E_q$  values calculated via the analytical representation of the solutions  $Q_q(t)$  by the Poincaré-Lindstedt series. The filled circles show a theoretical estimate based on the average energy of suitably defined groups of modes [see Eq. (35) and relevant discussion in the text].

this case, we find that the modes excited at the first order of the recursive scheme are  $q=5-12$ , while the modes excited at second order are  $q=13-16$  and the GALI method shows that the motion occurs on a four-torus since  $G_5$  is the first index to drop asymptotically like  $t^{-1}$  [see Fig. 2(d)].

The sequence of excitation of different modes plays demonstrably a crucial role in estimating the profile of energy localization since the amplitudes of all excited modes at the  $r$ th order have a prefactor  $\sigma^r = [\beta/2(N+1)]^r$ . This is the subject of the next section, in which a proposition is provided for the sequence of mode excitations, in the generic case of arbitrary  $N$  and arbitrary dimension  $s$  of the low-dimensional torus (with the restriction  $s < N$ ). Next, the consequences of this proposition are examined on the localization profile of  $q$ -tori and nearby FPU trajectories.

### C. Sequence of mode excitations

In order to motivate the results of this section, let us first limit ourselves to what happens in the case of the solutions of Figs. 1 and 2. Figure 3 shows the average harmonic energy of each mode over a time span  $T=10^6$  in the cases of the  $q$ -torus of Figs. 1 and 2, shown in Figs. 3(a) and 3(b), respectively. The numerical result (open circles) compares excellently with the analytical result (stars) obtained via the Poincaré-Lindstedt method. The filled circles in each plot represent “piecewise” estimates of the localization profile in groups of modes excited at consecutive orders of the recursive scheme. The derivation and exact meaning of these theoretical estimates will be analyzed in detail below. Here, we point out their main feature, showing a clear-cut separation of the modes into *groups* following essentially the sequence of excitations predicted by the Poincaré-Lindstedt series construction. Namely, in Fig. 3(a) we see clearly that the decrease in the average energy  $\bar{E}_q$  along the profile occurs by abrupt steps, with three groups formed by nearby energies, namely, the group of modes 1 and 2, then modes 3–6, and then modes 7 and 8. The same phenomenon is also seen in Fig. 3(b), where the grouping of the different modes follows

precisely the sequence of excitations (1–4), (5–12), (13–16) as predicted by the theory.

Let us, therefore, extend our approach to a more general consideration of the structure of the solutions lying on low-dimensional tori. Using the Poincaré-Lindstedt method, a solution and its frequencies are expanded in series of the form

$$Q_q(t) = \sum_{k=0}^{\infty} \sigma^k Q_q^{(k)}(t), \quad \omega_q = \sum_{k=0}^{\infty} \sigma^k \omega_q^{(k)}, \quad (23)$$

where  $\omega_q^{(0)} \equiv \Omega_q$ . Substituting Eq. (23) into the equations of motion (7) and separating terms of like orders, the equations at order  $k$  read

$$\begin{aligned} \ddot{Q}_q^{(k)} + \omega_q^2 Q_q^{(k)} &= \sum_{n_1=1}^k \left( \sum_{n_2=0}^{n_1} \omega_q^{(n_2)} \omega_q^{(n_1-n_2)} \right) Q_q^{(k-n_1)} \\ &\quad - \Omega_q \sum_{l,m,n=1}^N \Omega_l \Omega_m \Omega_n C_{qlmn} \\ &\quad \times \sum_{\substack{n_1, n_2, n_3=0 \\ n_1+n_2+n_3=k-1}}^{k-1} Q_l^{(n_1)} Q_m^{(n_2)} Q_n^{(n_3)}. \end{aligned} \quad (24)$$

Note that Eq. (24) is still quite general. Let us consider, therefore, the case where only a subset of modes  $1 \leq q_1 < q_2 < \dots < q_s \leq N$  is excited at the zeroth order of the perturbation theory, assuming that  $Q_q^{(0)} \neq 0$  if and only if  $q \in \{q_1, q_2, \dots, q_s\}$ . The modes  $q_1, \dots, q_s$  need not be consecutive. We wish to see how this type of zeroth-order excitation propagates at subsequent orders. More specifically, we wish to determine for which  $q$  values one has  $Q_q^{(k' < k)} = 0$ ,  $Q_q^{(k)} \neq 0$ , i.e., the modes  $q$  are first excited at the  $k$ th order. The answer is provided by the following.

*Proposition.* Let the starting terms of a Poincaré-Lindstedt series solution with  $s$  frequencies be set as

$$\begin{aligned} Q_{q_i}^{(0)} &= A_{q_i} \cos(\omega_{q_i} t + \phi_{q_i}) \quad \text{for } i = 1, 2, \dots, s, \quad 1 \leq q_1 \leq q_2 \\ &\leq \dots \leq q_s \leq N, \end{aligned}$$

$$Q_q^{(0)} = 0 \quad \text{for all } q \neq q_i. \quad (25)$$

Then, besides the terms  $Q_{q_i}^{(k)}(t)$ , the Poincaré-Lindstedt series terms  $Q_q^{(k)}(t)$  which are permitted to be nonzero at the  $k$ th order of the series expansion are given by the values of  $q = q^{(k)}$  satisfying

$$q^{(k)} = |2\lambda(N+1) - m_k|, \quad m_k[\text{mod}(N+1)] \neq 0, \quad (26)$$

where  $m_k$  can take any of the values  $|\pm q_{i_1} \pm q_{i_2} \pm \dots \pm q_{i_{2k+1}}|$ , with  $i_1, i_2, \dots, i_{2k+1} \in \{1, \dots, s\}$  for any possible combination of the  $\pm$  signs, and  $\lambda \equiv [(m_k + N)/2(N+1)]$ .

The proof of the proposition is given in Appendix A. Some simple examples clarify the use of rule (26):

*$q$  breathers.* If we excite only one mode  $q_1$  at zeroth order, new modes are excited one by one at subsequent orders and one has  $m_k = (2k+1)q_1$ . As long as  $m_k \leq N$ , the newly excited modes are  $q^{(k)} = m_k = (2k+1)q_1$ , i.e., exactly as predicted by Flach *et al.* [1]. A particular case arises when  $q_1 = 2(N+1)/3$ ,  $(N+1)/2$ , or  $(N+1)/3$ . Then, one readily sees that no new

modes are excited at any subsequent order, which is in agreement with a well-known result [36] (see also [37]).

*Two-dimensional q-tori.* Assume we excite the modes  $q_1 = 1, q_2 = 2$  at zeroth order. At first order ( $k=1$ ) we have again  $q = |q_{i_1} \pm q_{i_2} \pm q_{i_3}|$  with  $i_1, i_2, i_3 \in \{1, 2\}$ . We readily find that the newly excited modes are  $q=1+1+1=3, q=1+1+2=4, q=1+2+2=5$ , and  $q=2+2+2=6$ . At order  $k=2$ , the first newly excited mode is  $q=1+1+1+2+2=7$ , while the last newly excited mode is  $q=2+2+2+2+2=10$ . In general, at order  $k \geq 1$  the newly excited modes are  $2(2k-1)+1 \leq q \leq 2(2k+1)$ .

*s-dimensional q-tori.* Assume we excite the modes  $q_1 = 1, q_2 = 2, \dots, q_s = s$  at the zeroth order. In the same way as above we find that the newly excited modes at order  $k \geq 1$  are  $s(2k-1)+1 \leq q \leq s(2k+1)$ . More complicated choices of the initially excited modes  $q_1, \dots, q_s$  lead to very interesting localization patterns that will be the subject of a separate study.

#### D. Profile of the energy localization

In order to study now in Fourier space energy localization phenomena associated with FPU trajectories, let us construct estimates for all  $Q_q(t)$  terms participating in a particular  $q$ -torus solution in which the  $s$  first modes  $(q_1, q_2, \dots, q_s) = (1, 2, \dots, s)$  are excited at zeroth order of the theory, with amplitudes  $A_1, A_2, \dots, A_s$ , respectively.

Denoting by  $q^{(k)}$  the indices of all modes which are newly excited at  $k$ th order, according to the proposition of the previous section, one has

$$q^{(k)} \in \mathcal{M}_{s,k} \equiv \{\max[1, (2k-1)s+1], \dots, (2k+1)s\}. \tag{27}$$

Whence, the following useful estimates are obtained:

$$\forall q^{(k)} \in \mathcal{M}_{s,k} \quad (k \geq 1), \quad q^{(k)} \leq (2k+1)s, \tag{28}$$

$$\omega_{q^{(k)}} \lesssim \frac{(2k+1)\pi s}{N+1}.$$

Let us now define the ‘‘majorant’’ norm in the space of trigonometric polynomials  $f$ ,

$$\|f\| = \sum_{\mathbf{k}} |A_{\mathbf{k}}|, \tag{29}$$

where  $A_{\mathbf{k}}$  are the coefficients of a trigonometric polynomial with, say (for simplicity), only cosine terms,

$$f = \sum_{\mathbf{k}} A_{\mathbf{k}} \cos(\mathbf{k} \cdot \phi). \tag{30}$$

Quantity (29) satisfies all properties of the norm. Since the series terms of a mode  $Q_{q^{(k)}}(t)$  satisfy  $Q_{q^{(k)}}^{(n)} = 0, \forall n < k$ ,  $Q_{q^{(k)}}^{(k)} \neq 0$ , from Eq. (24) we deduce that the equation determining  $Q_{q^{(k)}}^{(k)}$  reads

$$\ddot{Q}_{q^{(k)}}^{(k)} + \omega_{q^{(k)}}^2 Q_{q^{(k)}}^{(k)} = -\Omega_{q^{(k)}} \sum_{\substack{n_1, 2, 3=0 \\ n_1+n_2+n_3=k-1}}^{k-1} \left( \sum_{(q^{(n_1)}, q^{(n_2)}, q^{(n_3)}) \in \mathcal{D}_{q^{(k)}}} \Omega_{q^{(n_1)}} \Omega_{q^{(n_2)}} \Omega_{q^{(n_3)}} Q_{q^{(n_1)}}^{(n_1)} Q_{q^{(n_2)}}^{(n_2)} Q_{q^{(n_3)}}^{(n_3)} \right), \tag{31}$$

where

$$\mathcal{D}_q = \{(q_{j_1}, q_{j_2}, q_{j_3}) : q \pm q_{j_1} \pm q_{j_2} \pm q_{j_3} = 0\}.$$

Assuming that the Lindstedt series are convergent, the omission of explicit reference to higher-order terms  $Q_{q^{(k)}}^{(k+1)}, Q_{q^{(k)}}^{(k+2)}, \dots$  is justified as long as only an estimate of the size of the oscillation amplitude of the mode  $q^{(k)}$  is sought.

The average size of the oscillation amplitudes of each mode along an  $s$ -dimensional  $q$ -torus follows now from estimates on the norms of the various terms appearing in Eq. (31). If we denote by  $A^{(k)}$  the mean value of all the norms  $\|Q_{q^{(k)}}\|$ , we find the following estimate:

$$A^{(k)} = \frac{(Cs)^k A_0^{2k+1}}{2k+1}, \tag{32}$$

where  $A_0 \equiv A^{(0)}$  is the mean amplitude of the oscillations of all modes excited at the zeroth order of the perturbation theory and  $C$  is a constant of order  $O(1)$ . The proof of Eq. (32) is deferred to Appendix B, in which the analytical estimate  $C \approx 3/2$  is given. In fact, Eq. (32) is a straightforward

generalization of the estimate given in Flach *et al.* [2] for  $q$  breathers, while the two estimates become identical (except for the precise value of  $C$ ) if one sets  $s=1$  in Eq. (32), and  $q_0=1$  in Flach’s  $q$ -breather formulae.

Thus, the  $q$ -tori provide an explanation for the results reported in [10,11] and offer a bridge between the natural packet approach and the interpretation of energy localization for FPU trajectories based on  $q$  breathers. In particular, the physical picture suggested by the above analysis is that, starting with initial conditions near  $q$  breathers, a ‘‘backbone’’ is formed in the phase space by a hierarchical set of solutions which are, precisely, the solutions lying on low-dimensional  $q$ -tori (of dimension  $s=1, 2, \dots, s \ll N$ ). All FPU trajectories with initial conditions within this set exhibit a profile of the energy localization characterized by a ‘‘stepwise’’ exponential decay, with step size equal to  $2s$ , as implied by Eq. (27). All the modes  $q^{(k)} \in \mathcal{M}_{k,s}$  share a nearly equal mean amplitude of oscillations, which follows the estimate of Eq. (32).

Using Eq. (32), we find it convenient to obtain piecewise estimates of the energy of each group using a formula for the average harmonic energies  $E^{(k)}$  of the modes  $q^{(k)}$ . To achieve

this, note that the total energy  $E$  given to the system can be estimated as the sum of the energies of the modes  $1, \dots, s$  (the remaining modes yield only small corrections to the total energy), i.e.,

$$E \sim s \omega_{q(0)}^2 A_0^2 \sim \frac{\pi^2 s^3 A_0^2}{(N+1)^2}.$$

On the other hand, the energy of each mode  $q^{(k)}$  can be estimated from

$$E^{(k)} \sim \frac{1}{2} \Omega_{q^{(k)}}^2 \left( \frac{\beta}{2(N+1)} \right)^{2k} (A^{(k)})^2 \sim \frac{\pi^2 s^2 (Cs\beta)^{2k} A_0^{4k+2}}{2^{2k+1} (N+1)^{2k+2}},$$

which, in terms of the total energy  $E$ , yields

$$E^{(k)} \sim \frac{E}{s} \left( \frac{C^2 \beta^2 (N+1)^2 E^2}{\pi^4 s^4} \right)^k. \quad (33)$$

Once again, the similarity of Eq. (33) with the corresponding equation for  $q$  breathers is obvious. The latter equation reads [2]

$$E_{(2k+1)q_0} \sim E_{q_0} \left( \frac{9\beta^2 (N+1)^2 E^2}{64\pi^4 q_0^4} \right)^k, \quad (34)$$

where  $q_0$  is the unique mode excited at zeroth order of the perturbation theory. Note, in particular, that the integer  $s$  plays in Eq. (33) a role similar to that of  $q_0$  in Eq. (34). This means that the energy profile of a  $q$  breather with  $q_0=s$  presents the same exponential law as the energy profile of the  $s$ -dimensional  $q$ -torus. But the most important feature of the latter type of solutions is that the profile remains *unaltered* as  $N$  increases, provided that (i) a constant fraction  $M=s/N$  of the spectrum is initially excited (i.e., that  $s$  increases proportionally to  $N$ ) and (ii) the *specific energy*  $\varepsilon=E/N$  remains constant. Indeed, in terms of the specific energy  $\varepsilon$ , Eq. (33) takes the form

$$E^{(k)} \sim \frac{\varepsilon}{M} \left( \frac{C^2 \beta^2 \varepsilon^2}{\pi^4 M^4} \right)^k, \quad (35)$$

i.e., the profile becomes *independent* of  $N$ . A similar behavior is recovered in the  $q$ -breather solutions provided that the “seed” mode  $q_0$  varies linearly with  $N$ , as was shown in detail in Refs. [38,39].

### E. Numerical results for FPU trajectories

Examples of the stepwise profiles predicted by Eq. (33) in the case of exact  $q$ -tori solutions are shown by filled circles in Fig. 3, concerning the solutions depicted in Figs. 1 and 2 (in all fittings we set  $C=1$  for simplicity). From these one can see that the theoretical piecewise profiles yield nearly the same average exponential slope as the profiles obtained either numerically or analytically by the construction of the solutions via the Poincaré-Lindstedt method. Thus, estimates (33) or (35) appear quite satisfactory for characterizing the localization profiles of exact  $q$ -tori solutions.

The key question now, regarding the relevance of the  $q$ -tori solutions for the interpretation of the FPU paradox, is whether Eq. (33) or Eq. (35) retains its predictive power in

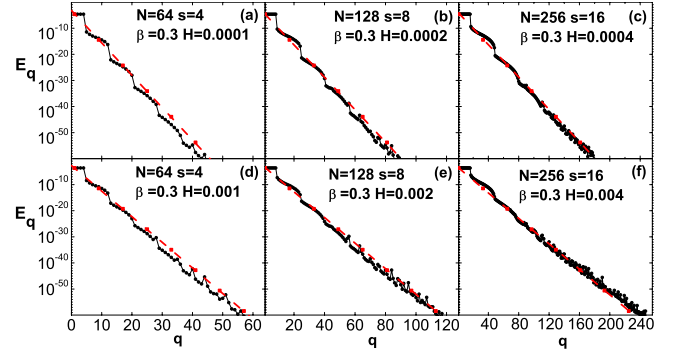


FIG. 4. (Color online) The average harmonic energy  $E_q$  of the  $q$ th mode over a time span  $T=10^6$  as a function of  $q$  in various examples of FPU trajectories, for  $\beta=0.3$ , in which the  $s(=N/16)$  first modes are only excited initially via  $Q_q(0)=A_q$ ,  $\dot{Q}_q(0)=0$ , and  $q=1, \dots, s$ , with  $A_q$  selected so that the total energy is equal to the value  $E=H$  indicated in each panel. We thus have (a)  $N=64$ ,  $E=10^{-4}$ ; (b)  $N=128$ ,  $E=2 \times 10^{-4}$ ; (c)  $N=256$ ,  $E=4 \times 10^{-4}$ ; (d)  $N=64$ ,  $E=10^{-3}$ ; (e)  $N=128$ ,  $E=2 \times 10^{-3}$ ; and (f)  $N=256$ ,  $E=4 \times 10^{-3}$ . The specific energy is constant in each of the two rows, i.e.,  $\varepsilon=1.5625 \times 10^{-6}$  in the top row and  $\varepsilon=1.5625 \times 10^{-5}$  in the bottom row. The dashed lines represent the average exponential profile  $E_q$  obtained theoretically by the hypothesis that the depicted FPU trajectories lie close to  $q$ -tori governed by profile (35).

the case of generic FPU trajectories which, by definition, are trajectories started close to, but not exactly, on a  $q$ -torus. An answer to this question is partly contained in the results presented in Figs. 4 and 5. Figure 4 shows the energy localization profile in numerical experiments in which  $\beta$  is kept fixed ( $\beta=0.3$ ), while  $N$  takes the values  $N=64, 128$ , and  $256$  (although in Sec. II B the derivation of explicit  $q$ -tori solutions was practically feasible by computer algebra only up to a rather small value of  $N$  ( $N=16$ ), in the present section the results with numerical trajectories are extended to much higher values of  $N$ ). In all six panels of Fig. 4 the FPU trajectories are computed starting with initial conditions in which *only* the  $s=4$  (for  $N=64$ ),  $s=8$  (for  $N=128$ ), and  $s=16$  (for  $N=256$ ) first modes are excited at  $t=0$ , with the

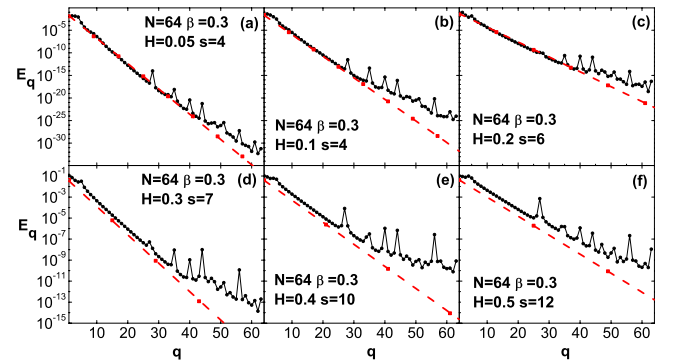


FIG. 5. (Color online) Same as in Fig. 4(a) but for larger energies, namely, (a)  $E=0.05$ , (b)  $E=0.1$ , (c)  $E=0.2$ , (d)  $E=0.3$ , (e)  $E=0.4$ , and (f)  $E=0.5$ . Beyond the threshold  $E \approx 0.05$ , theoretical profiles of form (33) yield the correct exponential slope if  $s$  is gradually increased from  $s=4$  in (a) and (b) to  $s=6$  in (c),  $s=7$  in (d),  $s=10$  in (e), and  $s=12$  in (f).

excitation amplitudes being compatible with the values of the total energy  $E$  indicated in each panel, and constant specific energy  $\varepsilon=1.5625 \times 10^{-6}$  in the top row and  $\varepsilon=1.5625 \times 10^{-5}$  in the bottom row of Fig. 4.

The resulting trajectories differ from  $q$ -tori solutions as follows: in the  $q$ -tori all modes have an initial excitation, whose size was estimated in Eq. (32) or Eq. (33), while in the case of the FPU trajectories only the  $s$  first modes are excited initially, and one has  $Q_q(0)=0$  for all modes  $q>s$ . Furthermore, since in the  $q$ -tori solutions one also has  $\|Q_{q>s}(t)\| \ll \|Q_{q \leq s}(t)\|$  for all  $t$ , the FPU trajectories can be considered as lying in the neighborhood of the  $q$ -torus solutions, at least initially. The numerical evidence is that if  $E$  is small, they remain close to the  $q$ -tori even after relatively long times, e.g.,  $t=10^6$ .

This is exemplified in Fig. 4, in which one sees that the average energy profiles of the FPU trajectories (at  $t=10^6$ ) exhibit the same behavior as predicted by Eq. (33), for an exact  $q$ -torus solution with the same total energy as the FPU trajectory in each panel. For example, based on the values of their average harmonic energy, the modes in Fig. 4(a) (in which  $s=4$ ) are clearly separated in groups (1–4), (5–12), and (13–20), etc., as foreseen by Eq. (27) for an exact four-torus solution. The energies of the modes in each group have a sigmoid variation around a level value characteristic of the group, which is nearly the value predicted by Eq. (33). The grouping of the modes is distinguishable in all the panels of Fig. 4; a careful inspection of which verifies that the grouping follows the laws found above for  $q$ -tori. Also, if we superpose the numerical data of the three top (or bottom) panels we find that the average exponential slope is nearly identical in all the panels of each row, a fact consistent with Eq. (35), according to which—for a given fraction  $M$  of initially excited modes—this slope depends on the specific energy only, i.e., it is independent of  $N$  for constant  $\varepsilon$ .

When we increase the energy, the FPU trajectories resulting from  $s$  initially excited modes start deviating from their associated exact  $q$ -tori solutions. As a consequence, the energy profiles of the FPU trajectories start also deviating from the energy profiles of the exact  $s$ -tori. This is evidenced by the fact that the profiles of the FPU trajectories become smoother, and the groups of modes become less distinct, while retaining the average exponential slope predicted by Eq. (35). This “smoothing” of the profiles is discernible in Fig. 5(a), in which the energy is increased by a factor of 50 with respect to Fig. 4(d), for the same values of  $N$  and  $\beta$ . Also, in Fig. 5(a) we observe the formation of the so-called “tail,” i.e., an overall rise of the localization profile at the high-frequency part of the spectrum, accompanied by spikes at particular modes. This is a precursor of the evolution of the system toward equipartition, which manifests itself earlier in time for larger energies.

Nevertheless, the important remark is that the phenomenon of exponential localization of the FPU trajectories persists and is still characterized by laws like Eq. (33), even when the energy is substantially increased. Furthermore, at energies beyond a threshold value, an interesting phenomenon occurs which is worth mentioning: for fixed  $N$  (see, e.g., Fig. 5, where  $N=64$ ), as the energy increases, a progressively higher value of  $s$  needs to be used in Eq. (33), so that

the theoretical profile yields an exponential slope that agrees with the numerical data.

As evidenced in Fig. 5 for  $\beta=0.3$ ,  $N=64$ , the threshold is  $E \approx 0.1$ . This value splits the system in two distinct regimes: one for  $E < 0.1$ , where the numerical data are well fitted by a constant choice of  $s=4$  in Eq. (33) (indicating that the FPU trajectories are indeed close to four-tori), and another for  $E > 0.1$ , where best-fit models of Eq. (33) occur for values of  $s$  increasing with the energy, e.g.,  $s=6$  for  $E=0.2$ , rising to  $s=12$  for  $E=0.5$ . This indicates that the respective FPU trajectories are close to  $q$ -tori with a progressively higher value of  $s$  (with  $s > 4$ ), despite the fact that only the four first modes are excited by the initial conditions of these trajectories.

This behavior is analogous to the natural packet scenario described by Berchiolla *et al.* [13], in which a set of modes is seen to share the energy after some time even if this energy is initially given to only the first mode. These authors also observed that the law giving the localization profile of their metastable states stabilizes as the energy increases. Indeed, according to Eq. (33), such a stabilization implies that in the second regime the width  $s$  depends asymptotically on  $E$  as  $s \propto E^{1/2}$  or from Eq. (35) that  $M \propto \varepsilon^{1/2}$ . This agrees well with estimates on the width of natural packets formed by the  $\beta$ -FPU model described in [12].

### III. STABILITY OF THE MOTION NEAR $q$ -TORI

#### A. Linear stability

The linear stability of  $q$  breathers can be studied by the implementation of Floquet theory (see [2]), which demonstrates that a  $q$  breather is linearly stable as long as

$$R = \frac{6\beta E_{q_0}(N+1)}{\pi^2} < 1 + O(1/N^2). \quad (36)$$

This result is obtained by analyzing the eigenvalues of the monodromy matrix of the linearized equations about a  $q$ -breather solution constructed by the Poincaré-Lindstedt series. Numerical verification can also be used to analyze the dynamics about the fixed point corresponding to a  $q$  breather under the Poincaré map of the flow of Eq. (7).

In the case of  $q$ -tori the above techniques are no longer available. Nevertheless, a reliable numerical criterion for the stability of  $q$ -tori is provided by the GALI indices [27]. According to this method, if a  $q$ -torus becomes unstable beyond a critical energy threshold, the deviation vectors of trajectories started exactly on the  $q$ -torus are attracted by its unstable manifold; whence, all the GALI indices beyond and including  $G_{k+1}$  ( $k$  being the dimension of the unstable manifold) fall exponentially fast. Naturally, if one starts with trajectories in the vicinity of an unstable  $q$ -torus, these trajectories are weakly chaotic. Thus, it turns out that all GALI indices start falling exponentially after a transient time, and this can be checked by calculating the time evolution of the lowest index, i.e.,  $G_2$ .

Using this criterion, we examined the stability of  $q$ -tori and determined approximately the value of the critical energy  $E_c$  at which a  $q$ -torus turns from stable to unstable.

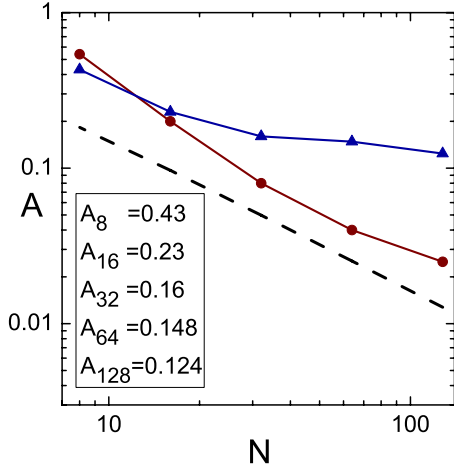


FIG. 6. (Color online) Assuming that the critical energy  $E_c$ , at which the GALI index  $G_2$  shows that a  $q$ -torus destabilizes is fitted by the law  $E_c = A\beta^{-1}$ , we show in the upper curve (triangles) the dependence of  $A$  on  $N$  for an FPU trajectory started by exciting initially only the  $q=1, 2$  modes. The middle curve (filled circles) corresponds to a similar calculation for FPU trajectories started near a  $q$ -breather solution, where only the  $q=1$  mode is excited. The dashed line corresponds to  $A \sim N^{-1}$ , according to the law of Eq. (36).

Figure 6 shows an example of this calculation using FPU trajectories started close to two-tori. The quantity  $A$  shown in the ordinate corresponds to a calculation keeping  $N$  fixed and varying  $\beta$ , until a critical energy  $E_c$  is determined, beyond which the GALI index  $G_2$  loses its asymptotically constant behavior. All calculations refer to a maximum time  $t_{max} = 10^7$  up to which we require that the exponential falloff of  $G_2$  must have been observed (in general  $E_c$  decreases as  $t_{max}$  increases, tending to an asymptotic limit as  $t_{max} \rightarrow \infty$ ). The values of  $E_c$  found this way provide *upper estimates* for the transition energy at which the exact  $q$ -torus turns from stable to unstable, i.e., for any choice of  $t_{max}$  the transition energy is *lower* than the value of  $E_c$  found by the GALI method.

As expected, due to the obvious scaling of the FPU Hamiltonian by  $\beta$ , the critical energy for all considered values of  $N$  turns out to be well fitted by a power law  $E_c = A\beta^{-1}$ . However, the fitting constant  $A$  depends also on  $N$ , as seen in Fig. 6. From the triangle data in the figure it is clear that the dependence of  $A$  on  $N$  is weaker than  $N^{-1}$ , i.e., the law predicted by Eq. (36) for the  $q$  breathers.

On the other hand, the dependence  $A \propto N^{-1}$  was approximately found for FPU trajectories started close to a  $q$  breather, where only the mode  $q=1$  is initially excited. In that case the numerical data (filled circles) have a slope close to that predicted by Eq. (36), although the whole numerical curve is shifted upward with respect to the dashed line, a fact verifying that the GALI method yields critical energies  $E_c$  which are *higher* than the value at which the  $q$  breather becomes unstable.

The weak dependence of  $A$  on  $N$  on the upper curve of Fig. 6 is a numerical indication that the  $q$ -tori solutions are *more robust* than the  $q$  breathers regarding their linear stability. This numerical behavior is related to the results of the previous section, which indicate that the number of modes

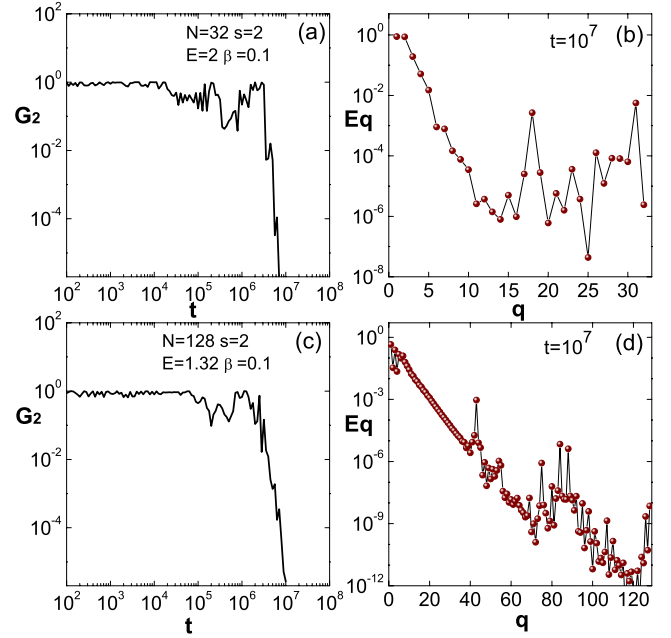


FIG. 7. (Color online) (a) Time evolution of the GALI index  $G_2$  up to  $t=10^7$  for an FPU trajectory started by exciting the  $q=1$  and 2 modes in the system  $N=32$ ,  $\beta=0.1$ , with a total energy  $E=2$ , i.e., higher than  $E_c=1.6$ . (b) *Instantaneous* localization profile of the FPU trajectory of (a) at  $t=10^7$ . (c) Same as in (a) but for  $N=128$ ,  $E=1.323$  (in this case the critical energy is  $E_c=1.24$ ). (d) Same as in (b) but for the trajectory of (c).

excited initially does not always coincide with the dimension of the  $q$ -torus which the FPU trajectory eventually approaches. Also, the destabilization of simple periodic orbit represented by a  $q$  breather does not imply that the tori surrounding the breather are also unstable.

At any rate, the most important remark concerning the linear stability of  $q$  breathers or  $q$ -tori is that the exponential localization of FPU trajectories persists even after the associated  $q$  breathers or  $q$ -tori have been identified as linearly unstable by the GALI criterion. This behavior is exemplified in Fig. 7, where Figs. 7(a) and 7(c) show the time evolution of the index  $G_2$  for two FPU trajectories started in the vicinity of two-tori of the  $N=32$  and  $N=128$  systems, when  $\beta=0.1$  and  $t_{max}=10^7$ . In both cases, the energy satisfies  $E > E_c$ , as the exponential falloff of the index  $G_2$  is already observed at  $t=10^7$ . However, a simple inspection of Figs. 7(b) and 7(d) clearly reveals that the exponential localization of the energy persists in the Fourier space of both systems. In fact we have found that the exponential localization persists for energies much larger than  $E_c$ , but for time scales which become smaller as  $E$  increases.

### B. Heuristic argument on exponential stability

The results of the previous section confirm the observation made on the basis of numerical experiments in [10] that a result establishing *exponential stability* for FPU trajectories close to  $q$ -tori should be possible. This has already been discussed in the Introduction, where we mentioned a partial result in this direction obtained recently in [17]. It was

pointed out, however, that so far the main obstruction to precise analytical statements lies in the bad dependence of all existing estimates on  $N$ .

Thus, in closing our paper, we would like to offer a heuristic argument on how the property of *exponential localization of the energy* for particular FPU trajectories could serve as a basis for further improvement of rigorous results. For definiteness, we refer below to the case of FPU trajectories for which the question of exponential stability can be examined in the framework of a variant of Birkhoff’s method due to Giorgilli [20], based on the direct calculation of approximate integrals of motion without the use of normal forms [40–42].

The trajectories we are referring to have initial conditions close to a particular family of  $q$ -breather solutions considered in [38,39], whose “seed mode”  $q_0$  varies proportionally to  $N$ . We thus take the seed mode to vary as  $q_0=(N+1)/2\mu$ , where  $\mu$  can be any large number that is a power of 2, while  $N$  is a power of 2 minus 1, so that no commensurabilities exist in the set of  $N$  unperturbed FPU frequencies  $\Omega_q$  (with  $q=1, \dots, N$ ). The exact  $q$ -breather solution oscillates with just one frequency and thus lies on a one-dimensional torus. However, perturbing this trajectory, we obtain solutions lying on  $\mu$ -dimensional tori involving the modes  $q=(2j-1)q_0$  (with  $j=1, 2, \dots, \mu$ ). Furthermore, the energy localization profile for the  $q$ -breather solution is the same as that of a  $s$ -dimensional  $q$ -torus solution with  $s=q_0$  given by Eq. (35), where  $M=q_0/N \approx 1/2\mu$ .

Let us assume that this localization profile holds also initially for the FPU trajectory that is a perturbation of the exact  $q$ -breather solution. Our aim then is to demonstrate that when one establishes estimates of exponential time of stability  $T \sim \exp(1/\varepsilon^c)$  for the energy localization profile of this type of FPU trajectories, the exponent  $c$  does not depend on the number of degrees of freedom (i.e., it is independent of  $\mu$ ), despite the Diophantine character of the unperturbed frequencies  $\Omega_q$  of the  $\mu$  modes  $q=(2j-1)q_0$  (with  $j=1, 2, \dots, \mu$ ).

To this end, we recall that, according to [20], the question of the long-term stability of particular trajectories can be examined by constructing approximate integrals of motion in the form of truncated series starting with harmonic energies

$$\Phi_j = \Phi_j^{(2)} + \Phi_j^{(4)} + \dots, \tag{37}$$

where  $\Phi_j^{(r)}$  is an  $r$ th degree polynomial in the canonical variables  $(q_1, \dots, q_N, p_1, \dots, p_N)$  defined by

$$q_j = \frac{\sqrt{\Omega_j} Q_j - iP_j/\sqrt{\Omega_j}}{\sqrt{2}}, \quad p_j = \frac{-i\sqrt{\Omega_j} Q_j + P_j/\sqrt{\Omega_j}}{\sqrt{2}}, \tag{38}$$

and  $\Phi_j^{(2)} \equiv E_j = i\Omega_j p_j q_j$ . The functions  $\Phi_j^{(r)}$  are determined recursively, by solving formally the Poisson bracket condition  $\{\Phi_j^{(2)} + \Phi_j^{(4)} + \dots, H_2 + H_4\} = 0$ , demanding that the series  $\Phi_j$  be an integral. Here,  $H_2$  and  $H_4$  are the quadratic and quartic terms of the  $\beta$ -FPU Hamiltonian written in the variables  $(q_j, p_j)$ . The order by order solution is then found via the so-called homological equation

$$\{\Phi_j^{(r-2)}, H_4\} + \{\Phi_j^{(r)}, H_2\} = 0, \quad r = 4, 6, \dots, \tag{39}$$

which has the same algebraic structure as the homological equation of Birkhoff’s normalization scheme. The solution reads

$$\Phi_j^{(r)} = - \sum_{\substack{m, n=1 \\ m+n=r}}^r \frac{h_{m,n}^{(r)} \mathbf{q}^m \mathbf{p}^n}{(\mathbf{m} - \mathbf{n}) \cdot \Omega}, \tag{40}$$

where the use is made of the compact notation  $\mathbf{q}^m \mathbf{p}^n \equiv q_1^{m_1} q_2^{m_2} \dots q_N^{m_N} p_1^{n_1} p_2^{n_2} \dots p_N^{n_N}$ ,  $\mathbf{m} \equiv (m_1, m_2, \dots, m_N)$ ,  $m \equiv m_1 + m_2 + \dots + m_N$  (similarly for  $\mathbf{n}$ ), and  $h_{m,n}^{(r)}$  are the polynomial coefficients of the Poisson bracket  $\{\Phi_j^{(r-2)}, H_4\}$ .

It is well known that the series (37) is asymptotic. We thus consider the  $r$ th order finite truncation  $\Phi_{j,r} = \Phi_j^{(2)} + \Phi_j^{(4)} + \dots + \Phi_j^{(r)}$  representing an *approximate* integral of motion whose time variation is given by

$$\frac{d\Phi_{j,r}}{dt} = R_{j,r} \equiv \{\Phi_{j,r}, H_4\}. \tag{41}$$

The quantity  $R_{j,r}$  is called the remainder function. The asymptotic character of the series implies that the size of  $R_{j,r}$  decreases initially as  $r$  increases, up to an optimal order  $r = r_{opt}$  beyond which the size of the remainder increases with  $r$ , becoming ultimately divergent as  $r \rightarrow \infty$ . Recursive application of the homological equation (39) (see [20,24] for details) yields that the size of the remainder at order  $r$  can be estimated by

$$\begin{aligned} \|R_{j,r}\| &\sim \frac{(r-2)\|R_{j,r-2}\|}{a_{r-2}} \\ &\sim \frac{(r-2)(r-4)\|R_{j,r-4}\|}{a_{r-2}a_{r-4}} \sim \dots \\ &\sim \frac{(r-2)! \|R_{j,4}\|}{a_{r-2}a_{r-4} \dots a_4}, \end{aligned} \tag{42}$$

where  $\|R_{j,r}\|$  denotes the absolute sum of the polynomial coefficients  $h_{m,n}$  for all  $(\mathbf{m}, \mathbf{n})$  with  $|\mathbf{m}| + |\mathbf{n}| = r$  and  $a_k$  ( $k = 4, 6, \dots, r-2$ ) denotes the minimum of all divisors  $(\mathbf{m} - \mathbf{n}) \cdot \Omega$ ,  $|\mathbf{m}| + |\mathbf{n}| = k$  at order  $k$ . The prefactors  $(r-2), (r-4), \dots$  come from the derivatives of the functions  $\Phi_j^{(r-2)}, \Phi_j^{(r-4)}, \dots$ , with respect to the canonical variables  $(\mathbf{q}, \mathbf{p})$ , appearing in Poisson brackets due to recursive application of the homological equation, which yield factors  $|\mathbf{m}|, |\mathbf{n}|$ , both of order  $O(r-2), O(r-4), \dots$  within the functions  $\Phi_j^{(r-2)}, \Phi_j^{(r-4)}, \dots, \Phi_j^{(4)}$ .

Our heuristic argument now goes as follows: since in the considered trajectories the total number of participating modes is equal to  $\mu$ , and  $N$  is a power of 2 minus 1, the associated divisors satisfy a *Diophantine condition* of the form

$$|\mathbf{l} \cdot \Omega| \geq \frac{\gamma}{|\mathbf{l}|^\tau} \quad \text{for all } \mathbf{l} \in \mathbb{Z}^N, \quad |\mathbf{l}| \neq 0 \tag{43}$$

with  $\tau > \mu - 1$ . The estimate  $\tau \sim \mu$  holds for  $\mu$  large. One then has  $a_{r-2}a_{r-4} \dots a_4 \sim \gamma^{(r-4)/2} (r-2)!^{-\mu}$ , which, upon substitution in Eq. (42) leads to

$$\|R_{j,r}\| \sim (r-2)! \mu^{+1} C_*^r \left(\frac{\beta}{N}\right)^{r/2}, \quad (44)$$

where the estimate  $\|H_4\| = O(\beta/N)$  is taken into account and  $C_*$  is a  $O(1)$  positive constant. These estimates, based on small divisors, are standard and lead by themselves to no improvement as far as the dependence of the asymptotic character on  $\mu$  is concerned. However, an improvement can be achieved if we also take into account the *numerators* of the remainder series, which for FPU trajectories possess the exponential localization profile shown in Eq. (34). In other words, the size of the remainder depends also on the size of the monomials

$$\Delta_\mu = (\Omega_1^{1/2} \xi_1)^{s_1} (\Omega_2^{1/2} \xi_2)^{s_2} \cdots (\Omega_\mu^{1/2} \xi_\mu)^{s_\mu},$$

where  $\xi_k$  stands for either  $q_k$  or  $p_k$  since each term of the remainder consists of one such a monomial multiplied by a coefficient bounded by an estimate of form (44). In view of Eq. (38), one has  $|\Omega_k^{1/2} \xi_k| \sim E_k^{1/2}$ . Thus, taking into account the form of profile (34), the size of the above monomial at the  $r$ th order of normalization can be estimated as

$$\begin{aligned} |\Delta_\mu| &\sim (E_1)^{s_1/2} (E_2)^{s_2/2} \cdots (E_\mu)^{s_\mu/2} \\ &\sim E^{(s_1+s_2+\cdots+s_\mu)/2} (\beta \mu^2 \varepsilon)^{s_2+2s_3+\cdots+(\mu-1)s_\mu}, \end{aligned}$$

where  $s_1+s_2+\cdots+s_\mu=r$ . For the leading terms (with smallest divisors) in the series the exponents  $s_1, s_2, \dots, s_\mu$  typically take values such that the estimate  $s_2+2s_3+\cdots+(\mu-1)s_\mu \sim \mu r/2$  holds. Thus,

$$|\Delta_\mu| \sim \mathcal{D}_*^r E^{r/2} \varepsilon^{\mu r/2} \quad (45)$$

where  $\mathcal{D}_*$  is a new constant. Combining now estimates (45) and (44) yields a final estimate for the size of the remainder of the form

$$\begin{aligned} \|R_r\| &\sim (r-2)! \mu^{+1} C_*^r \mathcal{D}_*^r \left(\frac{\beta}{N}\right)^{r/2} E^{r/2} \varepsilon^{\mu r/2} \\ &\sim |R_r| \sim \mathcal{B}_* [(r-2)!]^{(\mu+1)/2} \varepsilon^{(\mu+1)r/2}, \end{aligned} \quad (46)$$

The optimal order of truncation is found by taking the logarithm of Eq. (46), using Stirling's formula  $\ln n! \approx n \ln n - n$ , as well as  $r-2 \approx r$  (for  $r$  large), using  $d \ln \|R_r\| / dr \sim 0$ . We thus find  $r_{opt} \sim 1/\varepsilon$ ; whence, the optimal value of the remainder is

$$\|R_{opt}\| \sim \exp\left(-\frac{\mu+1}{2\varepsilon}\right), \quad (47)$$

i.e., the time variations of the integrals  $\Phi_{j,r_{opt}}$  are exponentially small in  $1/\varepsilon$ . This yields an estimate of exponential stability of the form  $T \sim \exp(1/\varepsilon^c)$ , where  $c=1$ , i.e., the number of degrees of freedom no longer appears in the exponent  $c$ . Compared to general estimates yielding  $c \sim 1/\mu$ , it is seen that the removal of the dependence of  $c$  on  $\mu$  was possible thanks to the assumed *exponential scaling* of the energy localization profile that allows for estimate (45). In turn, since this localization profile is the same as for  $q$ -tori, the above analysis is suggestive of the usefulness of exponential localization in the  $q$  space in order to obtain improved estimates in the case of  $q$ -tori solutions as well. However, in the lack of

a rigorous demonstration, it remains an open question whether such a strategy can lead to estimates of a stretched exponential law for the dependence of  $\|R_{opt}\|$  on  $\varepsilon$ , as evidenced also to a limited extent by the numerical experiments of [10].

#### IV. CONCLUSIONS

The main conclusions of the present study can be summarized as follows:

(1) We introduced the concept of  $q$ -tori in FPU lattices, which represent a generalization of the concept of  $q$  breathers. The  $q$ -tori have low dimensionality  $s \ll N$  and arise from the continuation of motions with  $s$  independent frequencies of the unperturbed problem.

(2) We explicitly calculated FPU solutions lying on  $q$ -tori by employing the method of the Poincaré-Lindstedt series. Based on estimates of the leading terms of these series, we provided a theoretical law yielding the average exponential localization of the energy in Fourier space for solutions on  $q$ -tori. Furthermore, a proposition was proved which explains how different groups of modes are excited at consecutive orders of the perturbation theory. The most important conclusion from this analysis is that, if the fraction  $s/N$  is kept constant, it appears that the localization profile depends on the *specific energy*  $\varepsilon = E/N$  of the system, i.e., it is independent of  $N$ . Some numerical evidence is provided in support of the above theoretical analysis, but further numerical work is necessary, in order to clarify the extent of its validity.

(3) We explored numerically the relevance of  $q$ -tori of dimension  $s$  to the dynamics of FPU trajectories started nearby, by exciting  $s$  modes only. The localization laws found analytically for  $q$ -tori accurately describe the localization of energy in Fourier space for the FPU trajectories as well. We also gave numerical evidence of the existence of two regimes separated by a critical energy value. Below this energy, the localization profiles  $E(q) \propto \exp(-bq)$  have a slope  $b$  depending logarithmically on  $\varepsilon$ , while the fraction  $M = s/N$  of modes sharing the energy is constant. Furthermore, beyond this critical energy the slope of the localization profile tends to stabilize, and  $M$  tends asymptotically to the law  $M \propto \varepsilon^{1/2}$ , as  $q$ -tori of progressively higher dimension begin to describe the dynamics of the numerical FPU trajectories.

(4) We examined the stability of  $q$ -tori using a numerical criterion provided by the GALI indices [27] and provided numerical evidence demonstrating that the localization in Fourier space persists for energies well above the threshold value at which the underlying  $q$ -tori turn from stable to unstable.

(5) Finally, we provided a heuristic argument suggesting that the exponential energy localization in  $q$ -mode space implies a particular analytical structure of the Birkhoff series obtained for associated FPU trajectories that could lead to improved estimates of the long-term stability in the spirit of the Nekhoroshev theory. In the example of FPU trajectories started close to  $q$ -breather solutions exhibiting the same energy localization as for  $q$ -tori, our arguments suggest that in stability estimates of the form  $T \sim \exp(1/\varepsilon^c)$  it is possible to remove the bad dependence of  $c$  on the number of degrees of

freedom of the problem. Of course, further study, substantiated by numerical experiments, is needed before rigorous statements become available on this issue.

### ACKNOWLEDGMENTS

We wish to thank Dr. S. Flach, Dr. A. Ponomorov, and Dr. A. Giorgilli for useful discussions clarifying particular points of the paper, as well as one referee who pointed out some inconsistencies in our first version. H.C. was supported in part by a grant from I.K.Y., the Foundation of State Scholarships of Greece, and gratefully acknowledges the hospitality of the Max Planck Institute for the Physics of Complex Systems.

### APPENDIX A: SEQUENCE OF MODE EXCITATIONS

For all  $q \neq q_i$  (with  $i=1, \dots, s$ ), the equations yielding the Poincaré-Lindstedt series terms  $\mathcal{Q}_q^{(1)}$  at first order are

$$\ddot{\mathcal{Q}}_q^{(1)} + \Omega_q^2 \mathcal{Q}_q^{(1)} = - \sum_{l,m,n=1}^N \Omega_q \Omega_l \Omega_m \Omega_n C_{qlmn} \mathcal{Q}_l^{(0)} \mathcal{Q}_m^{(0)} \mathcal{Q}_n^{(0)}. \quad (\text{A1})$$

The r.h.s. of the above equations is different from zero if  $C_{qlmn} \neq 0$ . In view of definition (6) of  $C_{qlmn}$ , nonzero solutions of Eq. (A1) containing no new frequencies  $\Omega_q$  are possible for the values of  $q$  satisfying either  $q=q^{(1)} = |\pm l \pm m \pm n| = m_1$  with  $l, m, n \in \{q_1, q_2, \dots, q_s\}$ , when  $1 \leq m_1 \leq N$ , or  $q^{(1)} = |2(N+1) - |\pm l \pm m \pm n||$ , when  $N+2 \leq m_1 \leq 2N+1$  or  $2N+3 \leq m_1 \leq 3N$ . Both cases are given by Eq. (26), for  $\lambda=0$  and 1, respectively. Thus, the proposition holds for  $k=1$ . Assuming it to be true at order  $k-1$ , and using Eq. (31), one finds for the  $k$ th order that solutions introducing no new frequencies are possible for the modes satisfying either  $q=q^{(k)} = |\pm l \pm m \pm n|$  (with  $1 \leq q^{(k)} \leq N$ ) or  $q=q^{(k)} = |2(N+1) - m_1|$  (with  $1 \leq q^{(k)} \leq N$ ), where

$$l = |2\lambda_{n_1}(N+1) - m_{n_1}|,$$

$$m_{n_1} = |q_{j_1} \pm q_{j_2} \pm \dots \pm q_{j_{2n_1+1}}|, \quad \lambda_{n_1} = \left\lceil \frac{m_{n_1} + N}{2(N+1)} \right\rceil,$$

$$m = |2\lambda_{n_2}(N+1) - m_{n_2}|, \quad m_{n_2} = |q_{r_1} \pm q_{r_2} \pm \dots \pm q_{r_{2n_2+1}}|,$$

$$\lambda_{n_2} = \left\lceil \frac{m_{n_2} + N}{2(N+1)} \right\rceil,$$

$$n = |2\lambda_{n_3}(N+1) - m_{n_3}|, \quad m_{n_3} = |q_{t_1} \pm q_{t_2} \pm \dots \pm q_{t_{2n_3+1}}|,$$

$$\lambda_{n_3} = \left\lceil \frac{m_{n_3} + N}{2(N+1)} \right\rceil, \quad (\text{A2})$$

with  $j_1, \dots, j_{2n_1+1}, r_1, \dots, r_{2n_2+1}, t_1, \dots, t_{2n_3+1} \in \{1, \dots, s\}$ ,  $n_1 + n_2 + n_3 = k-1$ . Taking the last relation as well as all possible sign combinations in the sum  $\pm l \pm m \pm n$  into account, the

permitted modes at  $k$ th order are given by equations of the form

$$q^{(k)} = |2(\pm \lambda_{n_1} \pm \lambda_{n_2} \pm \lambda_{n_3} \pm g)(N+1) + (\pm q_{i_1} \pm q_{i_2} \pm \dots \pm q_{i_{2k+1}})|, \quad (\text{A3})$$

provided that  $1 \leq q^{(k)} \leq N$ , where  $g=0$  or 1, and  $i_1, i_2, \dots, i_{2k+1} \in \{1, \dots, s\}$ . After a possible sign reversal within  $|\cdot|$ , not affecting the absolute value, the expression

$$q^{(k)} = |2(\pm \lambda_{n_1} \pm \lambda_{n_2} \pm \lambda_{n_3} \pm g)(N+1) + (\pm q_{i_1} \pm q_{i_2} \pm \dots \pm q_{i_{2k+1}})|$$

always resumes the form

$$q^{(k)} = |2\lambda(N+1) - m_k|, \quad (\text{A4})$$

where  $m_k = |q_{i_1} \pm q_{i_2} \pm \dots \pm q_{i_{2k+1}}|$  and  $\lambda$  is an integer number. However, by the second restriction of Eq. (A3), namely,  $1 \leq q^{(k)} \leq N$ , one necessarily has that  $\lambda = [(m_k + N)/2(N+1)]$ , which concludes the proof of the proposition.

### APPENDIX B: ESTIMATES ON LOCALIZATION PROFILES

The products  $\mathcal{Q}_{q^{(n_1)}}^{(n_1)} \mathcal{Q}_{q^{(n_2)}}^{(n_2)} \mathcal{Q}_{q^{(n_3)}}^{(n_3)}$  in Eq. (31) give rise to trigonometric terms of the form

$$\mathcal{Q}_{q^{(n_1)}}^{(n_1)} \mathcal{Q}_{q^{(n_2)}}^{(n_2)} \mathcal{Q}_{q^{(n_3)}}^{(n_3)} \rightarrow \cos(a_1 \omega_1 + a_2 \omega_2 + \dots + a_s \omega_s) t: \\ a_i \in \mathcal{Z}, \quad |a_1| + |a_2| + \dots + |a_s| \leq 2k+1 \quad (\text{B1})$$

on the r.h.s. of Eq. (31). For each trigonometric term of form (B1), and  $k \geq 1$ , Eq. (31) introduces a divisor to the solution for  $\mathcal{Q}_{q^{(k)}}^{(k)}$ , namely,

$$\Omega_{q^{(k)}}^2 - \left( \sum_{j=1}^s a_j \omega_j \right)^2 = \left( \Omega_{q^{(k)}} - \sum_{j=1}^s a_j \omega_j \right) \left( \Omega_{q^{(k)}} + \sum_{j=1}^s a_j \omega_j \right). \quad (\text{B2})$$

In view of Eq. (22), the smallest divisors are those satisfying

$$q^{(k)} = \sum_{j=1}^s a_j j. \quad (\text{B3})$$

For such divisors, one has

$$\omega_{q^{(k)}} - \sum_{j=1}^s a_j \omega_j = \frac{\pi^3 \left( (q^{(k)})^3 - \sum_{j=1}^s a_j j^3 \right)}{24(N+1)^3} + O((\pi s k/N)^5),$$

while, for the sum  $\sum_{j=1}^s a_j j^3$  one has the inequality

$$\left| \sum_{j=1}^s a_j j^3 \right| \leq \sum_{j=1}^s |a_j| \cdot \sum_{j=1}^s j^3 = \sum_{j=1}^s |a_j| \cdot \frac{s^2(s+1)^2}{4}$$

in view of which the estimate

$$\left| \sum_{j=1}^s a_j j^3 \right| \sim \frac{s^4 \sum_{j=1}^s |a_j|}{4}$$

holds. On the other hand, using condition (B3) as well as Eq. (28) one obtains

$$(2k+1)s \sim \sum_{j=1}^s |a_j| \cdot \sum_{j=1}^s j \sim \frac{s^2}{2} \sum_{j=1}^s |a_j|.$$

Combining the last two expressions we find

$$\left| \sum_{j=1}^s a_j j^3 \right| \sim \frac{s^3(2k+1)}{2}$$

in view of which [combined with Eq. (28)] one finally arrives at an estimate for the size of divisors

$$\begin{aligned} & \left| \omega_{q^{(k)}} - \sum_{j=1}^s a_j \omega_j \right| \left| \omega_{q^{(k)}} + \sum_{j=1}^s a_j \omega_j \right| \\ & \sim \frac{\pi^3 s^3 (2k+1) \left[ (2k+1)^2 - \frac{1}{2} \right] 2\pi s (2k+1)}{24(N+1)^3 (N+1)} \\ & \sim \frac{\pi^4 s^4 (2k+1)^4}{12(N+1)^4}. \end{aligned} \quad (\text{B4})$$

Returning to Eq. (31), for fixed values of  $n_1, n_2$ , and  $n_3$ , there are at most  $s$  triplets  $(q^{(n_1)}, q^{(n_2)}, q^{(n_3)})$  satisfying  $(q^{(n_1)}, q^{(n_2)}, q^{(n_3)}) \in \mathcal{D}_{q^{(k)}}$ . Using this fact as well as estimates (B4) and (28), one obtains for the norms of the various terms the estimate

$$\begin{aligned} \|\mathcal{Q}_{q^{(k)}}^{(k)}\| & \sim \frac{12(N+1)^4}{\pi^4 s^4 (2k+1)^4} \frac{\pi s (2k+1)}{(N+1)} \frac{s^4 \pi^3}{(N+1)^3} \\ & \times \sum_{\substack{n_{1,2,3}=0 \\ n_1+n_2+n_3=k-1}}^{k-1} (2n_1+1)(2n_2+1)(2n_3+1) \|\mathcal{Q}_{q^{(n_1)}}^{(n_1)}\| \\ & \times \|\mathcal{Q}_{q^{(n_2)}}^{(n_2)}\| \|\mathcal{Q}_{q^{(n_3)}}^{(n_3)}\| \end{aligned}$$

or

$$\begin{aligned} \|\mathcal{Q}_{q^{(k)}}^{(k)}\| & \sim \frac{12s}{(2k+1)^3} \sum_{\substack{n_{1,2,3}=0 \\ n_1+n_2+n_3=k-1}}^{k-1} (2n_1+1)(2n_2+1)(2n_3+1) \\ & \times \|\mathcal{Q}_{q^{(n_1)}}^{(n_1)}\| \|\mathcal{Q}_{q^{(n_2)}}^{(n_2)}\| \|\mathcal{Q}_{q^{(n_3)}}^{(n_3)}\|. \end{aligned} \quad (\text{B5})$$

Denoting by  $A^{(k)}$  the average size of the oscillations of all the modes  $q^{(k)}$ , Eq. (B5) takes the form

$$\begin{aligned} A^{(k)} & = \frac{12s}{(2k+1)^3} \sum_{\substack{n_{1,2,3}=0 \\ n_1+n_2+n_3=k-1}}^{k-1} (2n_1+1)(2n_2+1)(2n_3+1) A^{(n_1)} A^{(n_2)} A^{(n_3)}. \end{aligned} \quad (\text{B6})$$

By induction it now follows that

$$A^{(n)} \simeq \frac{(3s/2)^n A_0^{2n+1}}{2n+1}. \quad (\text{B7})$$

Indeed, assuming Eq. (B7) to be true for the amplitudes  $A^{(n_1)}$ ,  $A^{(n_2)}$ , and  $A^{(n_3)}$  in Eq. (B6), it follows that

$$\begin{aligned} A^{(k)} & \simeq \frac{(3s/2)^{k-1} 12s A_0^{2k+1}}{(2k+1)^3} \sum_{\substack{n_{1,2,3}=0 \\ n_1+n_2+n_3=k-1}}^{k-1} 1 \\ & = \frac{(3s/2)^{k-1} 12s A_0^{2k+1}}{(2k+1)^3} \frac{k(k+1)}{2} \\ & \simeq \frac{(3s/2)^{k-1} 12s A_0^{2k+1}}{(2k+1)^3} \frac{(2k+1)^2}{8} = \frac{(3s/2)^k A_0^{2k+1}}{2k+1}, \end{aligned}$$

which demonstrates the validity of Eq. (32) in the text, with the constant  $C$  having the specific value  $C=3/2$ .

- 
- [1] S. Flach, M. V. Ivanchenko, and O. I. Kanakov, Phys. Rev. Lett. **95**, 064102 (2005).  
[2] S. Flach, M. V. Ivanchenko, and O. I. Kanakov, Phys. Rev. E **73**, 036618 (2006).  
[3] S. Flach and A. Ponomorov, Physica D **237**, 908 (2008).  
[4] E. Fermi, J. Pasta, and S. Ulam, Los Alamos National Laboratory Report No. LA-1940, 1955 reproduced in Lect. Notes Math. **15**, 143 (1974).  
[5] S. Flach and A. Gorbach, Phys. Rep. **467**, 1 (2008).  
[6] L. Galgani and A. Scotti, Phys. Rev. Lett. **28**, 1173 (1972).  
[7] F. Fucito, F. Marchesoni, E. Marinari, G. Parisi, L. Politi, S. Ruffo, and A. Vulpiani, J. Phys. (Paris) **43**, 707 (1982).  
[8] R. Livi, M. Pettini, S. Ruffo, and A. Vulpiani, Phys. Rev. A **31**, 2740 (1985).  
[9] J. De Luca, A. Lichtenberg, and M. Lieberman, Chaos **5**, 283 (1995).  
[10] L. Berchialla, L. Galgani, and A. Giorgilli, Phys. Lett. A **321**, 167 (2004).  
[11] J. De Luca, A. J. Lichtenberg, and S. Ruffo, Phys. Rev. E **60**, 3781 (1999).  
[12] A. Lichtenberg, R. Livi, M. Pettini, and S. Ruffo, Lect. Notes Phys. **728**, 21 (2008).  
[13] L. Berchialla, L. Galgani, and A. Giorgilli, Discrete Contin. Dyn. Syst., Ser. A **11**, 855 (2005).

- [14] G. Benettin, A. Carati, L. Galgani, and A. Giorgilli, *Lect. Notes Phys.* **728**, 151 (2008).
- [15] A. Ponno and D. Bambusi, *Chaos* **15**, 015107 (2005).
- [16] D. Bambusi and A. Ponno, *Commun. Math. Phys.* **264**, 539 (2006).
- [17] A. Giorgilli and D. Muraro, *Boll. Unione Mat. Ital. B* **9**, 1 (2006).
- [18] N. Nekhoroshev, *Russ. Math. Surveys* **32**, 1 (1977).
- [19] G. Benettin, L. Galgani, and A. Giorgilli, *Celest. Mech.* **37**, 1 (1985).
- [20] A. Giorgilli, *Ann. Inst. Henri Poincaré, Sect. A* **48**, 423 (1988).
- [21] F. Fassó, M. Guzzo, and G. Benettin, *Commun. Math. Phys.* **197**, 347 (1998).
- [22] M. Guzzo, F. Fassó, and G. Benettin, *Math. Phys. Electron. J.* **4**, 1 (1998).
- [23] L. Niederman, *Nonlinearity* **11**, 1465 (1998).
- [24] C. Efthymiopoulos, A. Giorgilli, and G. Contopoulos, *J. Phys. A* **37**, 10831 (2004).
- [25] A. Giorgilli, in *Hamiltonian Dynamical Systems*, edited by K. Meyer, D. Schmidt, I. Cincinati, and S. Dumas (Springer, Berlin, 1992).
- [26] G. Benettin, L. Galgani, and A. Giorgilli, *Phys. Lett. A* **120**, 23 (1987).
- [27] C. Skokos, T. Bountis, and C. Antonopoulos, *Physica D* **231**, 30 (2007).
- [28] P. Hemmer, *Det Physiske Seminar i Trondheim* **2**, 66 (1959).
- [29] B. Rink, *Commun. Math. Phys.* **218**, 665 (2001).
- [30] A. Giorgilli, *Planet. Space Sci.* **46**, 1441 (1998).
- [31] L. Eliasson, *Math. Phys. Electron. J.* **2**, 1 (1997).
- [32] G. Gallavotti, *Commun. Math. Phys.* **164**, 145 (1994).
- [33] G. Gallavotti, *Rev. Math. Phys.* **6**, 343 (1994).
- [34] A. Giorgilli, in *Hamiltonian Systems of Three or More Degrees of Freedom*, edited by C. Simo (Kluwer, Dordrecht, 1999).
- [35] A. Giorgilli and U. Locatelli, *ZAMP* **48**, 220 (1997).
- [36] R. L. Bivins, N. Metropolis, and J. Pasta, *J. Comput. Phys.* **12**, 65 (1973).
- [37] C. Antonopoulos and T. Bountis, *Phys. Rev. E* **73**, 056206 (2006).
- [38] S. Flach, O. Kanakov, M. Ivanchenko, and K. Mishagin, *Int. J. Mod. Phys. B* **21**, 3925 (2007).
- [39] O. Kanakov, S. Flach, M. Ivanchenko, and K. Mishagin, *Phys. Lett. A* **365**, 416 (2007).
- [40] E. T. Whittaker, *Proc. R. Soc. Edinburgh* **37**, 95 (1916).
- [41] T. M. Cherry, *Proc. Cambridge Philos. Soc.* **22**, 510 (1924).
- [42] G. Contopoulos, *Z. Astrophys.* **49**, 273 (1960).